AD-A080 551 FAIRLEIGH DICKINSON UNIV TEANECK NJ DEPT OF PHYSICS F/G 20/6
SURVEY OF INFRARED ABSORPTION PHENOMENA AND EXPERIMENTAL METHOD--ETC(U)
SEP 79 K D MOELLER, V P TOMASELLI DAAK10-77-C-0121
UNCLASSIFIED FDU-1 ARCSL-CR-79052 NL

| OF |
AD
A080551

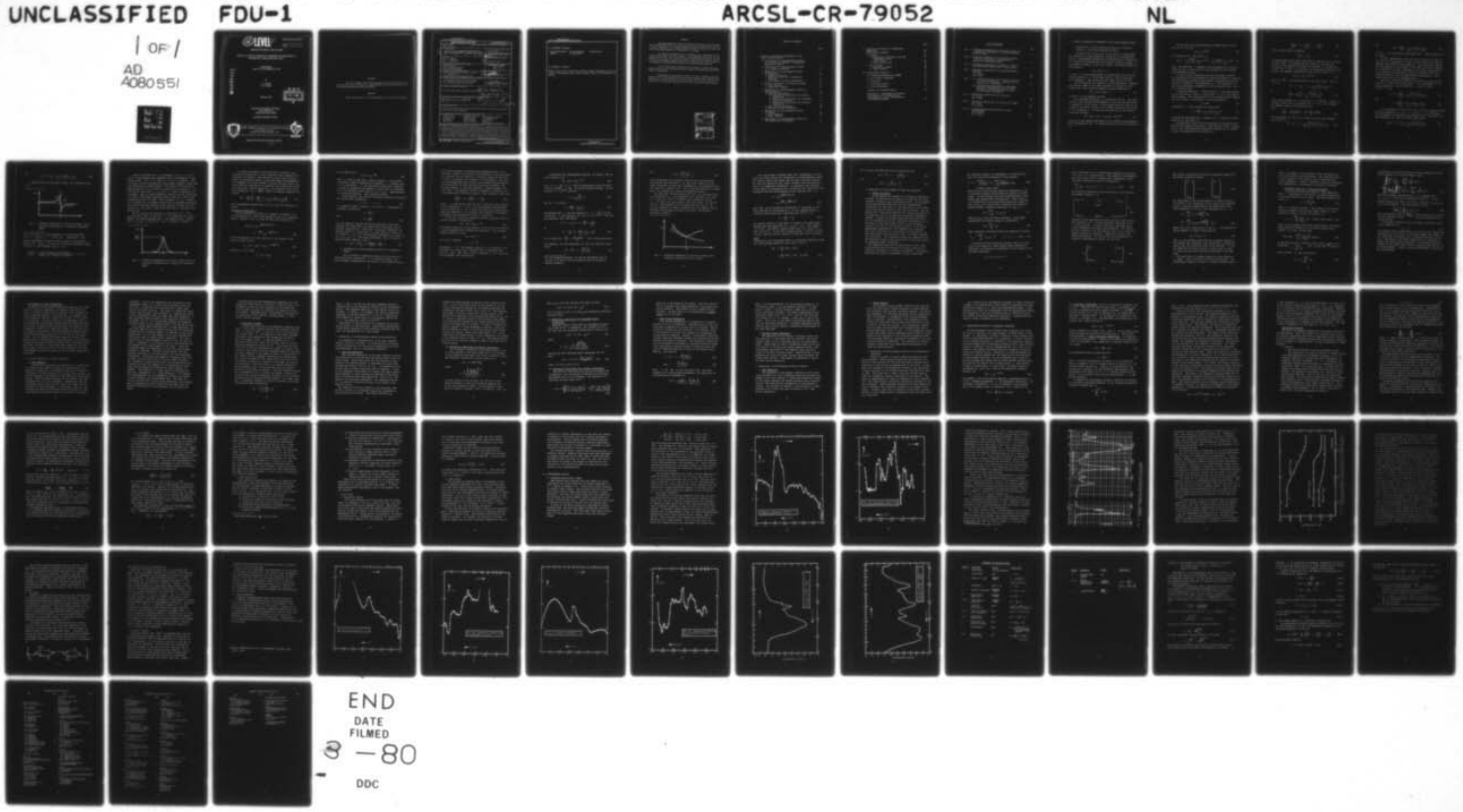

END
DATE
FILMED
3 -80
DDC

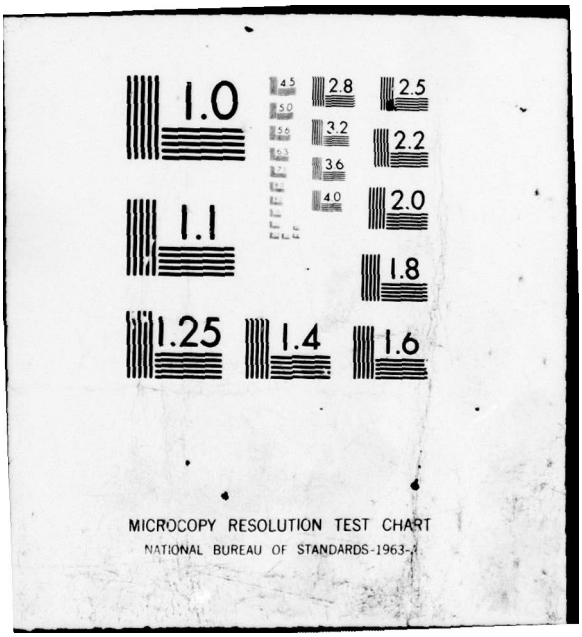
1.0
1.1
1.25
1.4
1.6
1.8
2.0
2.2
2.5
2.8
3.2
3.6
4.0
4.5
5.0
5.6
MICROCOPY RESOLUTION TEST CHART
NATIONAL BUREAU OF STANDARDS-1963-A

(12) LEVEL III

AD-E410222

AD

CONTRACTOR REPORT ARCSL-CR-79052

SURVEY OF INFRARED ABSORPTION PHENOMENA AND EXPERIMENTAL METHODS FOR LIQUIDS AND SOLID FILMS

Progress Report
June 15, 1977 to September 15, 1977

by

K. D. Moeller
V. P. Tomaselli

September 1979

FAIRLEIGH DICKINSON UNIVERSITY
Physics Department
Teaneck, New Jersey 07666

Contract No. DAAK10-77-C-0121

US ARMY ARMAMENT RESEARCH AND DEVELOPMENT COMMAND
Chemical Systems Laboratory
Aberdeen Proving Ground, Maryland 21010

Disclaimer

The views, opinions, and/or findings contained in this report are those of the authors and should not be construed as an official Department of the Army position, policy, or decision unless so designated by other documentation.

Disposition

Destroy this report when it is no longer needed. Do not return it to the originator.

UNCLASSIFIED

SECURITY CLASSIFICATION OF THIS PAGE *(When Data Entered)*

REPORT DOCUMENTATION PAGE

READ INSTRUCTIONS BEFORE COMPLETING FORM

1. REPORT NUMBER: ARCSL-CR-79052
2. GOVT ACCESSION NO.:
3. RECIPIENT'S CATALOG NUMBER:

4. TITLE *(and Subtitle)*: SURVEY OF INFRARED ABSORPTION PHENOMENA AND EXPERIMENTAL METHODS FOR LIQUIDS AND SOLID FILMS

5. TYPE OF REPORT & PERIOD COVERED: Progress Report, June 15 - September 15, 1977

6. PERFORMING ORG. REPORT NUMBER: FDU-1

7. AUTHOR(s): K. D. Moeller, V. P. Tomaselli

8. CONTRACT OR GRANT NUMBER(s): DAAK10-77-C-0121

9. PERFORMING ORGANIZATION NAME AND ADDRESS:
Physics Department
Fairleigh Dickinson University
Teaneck, New Jersey 07666

10. PROGRAM ELEMENT, PROJECT, TASK AREA & WORK UNIT NUMBERS: 12 71L

11. CONTROLLING OFFICE NAME AND ADDRESS:
Commander/Director, Chemical Systems Laboratory
Attn: DRDAR-CLJ-R
Aberdeen Proving Ground, Maryland 21010

12. REPORT DATE: Sept[illegible]79

13. NUMBER OF PAGES: 71

14. MONITORING AGENCY NAME & ADDRESS *(if different from Controlling Office)*:
Commander/Director, Chemical Systems Laboratory
Attn: DRDAR-CLB-PS/Dr. Edward W. Stuebing
Aberdeen Proving Ground, Maryland 21010

15. SECURITY CLASS. *(of this report)*: UNCLASSIFIED

15a. DECLASSIFICATION/DOWNGRADING SCHEDULE: NA

16. DISTRIBUTION STATEMENT *(of this Report)*

Approved for public release, distribution unlimited.

19 CR-79052, AD-E 410 222

17. DISTRIBUTION STATEMENT *(of the abstract entered in Block 20, if different from Report)*

18 ARCSL, SBIE

9 Progress Rept. 15 Jun-15 Sep 77,

18. SUPPLEMENTARY NOTES

This study was sponsored by the Army Smoke Research Program, Chemical Systems Laboratory, Aberdeen Proving Ground, Maryland.

19. KEY WORDS *(Continue on reverse side if necessary and identify by block number)*

Infrared spectra	Absorption coefficient	Molar extinction coefficient
Optical constants	Refractive index	Electromagnetic wave
Attenuation	Lattice vibrations	Semiconductors
Metal powders	Dielectric powders	Beer's Law

(continued on reverse side)

20. ABSTRACT *(Continue on reverse side if necessary and identify by block number)*

A discussion of absorption phenomena in the infrared (2.5 to 15 micrometers) spectral region is presented. Mechanisms surveyed include the attenuation of electromagnetic waves by dielectrics and metals; molecular absorption processes; lattice vibrations in bulk and powdered dielectrics; band gap, free carrier and multiple phonon absorption in semiconductors; absorption in bulk and powdered metals; and absorption by polymeric one-dimensional conductors. Also presented is a review of quantitative methods of determining the optical constants of solids, liquids and gases and their

(continued on reverse side)

DD FORM 1 JAN 73 1473 EDITION OF 1 NOV 65 IS OBSOLETE

UNCLASSIFIED 403 665

SECURITY CLASSIFICATION OF THIS PAGE *(When Data Entered)*

19. KEYWORDS (Continued)

Polymethylmethacrylate	Tri-n-butyl phosphate	Polyvinyl alcohol
Cellulose	Ureaformaldehyde	

20. ABSTRACT (Continued)

possible sources of error. The results of quantitative absorption measurements on tri-n-butyl phosphate, polymethylmethacrylate, cellulose, polyvinyl alcohol, and ureaformaldehyde are included.

PREFACE

This report describes the effort in the infrared spectral region. It covers the period June 15 through September 15, 1977 and was performed under Contract DAAK10-77-C-0121 by the Physics Department of the Fairleigh Dickinson University in Teaneck, New Jersey. The research was conducted jointly by K. D. Moeller and V. P. Tomaselli

The research was initiated by Dr. E. W. Stuebing of the Aerosol Sciences Team, Applied Sciences Division, US Army, Frankford Arsenal, Philadelphia, Pennsylvania, and was sponsored by the Army Smoke Research Program, Chemical Systems Laboratory, Aberdeen Proving Ground, Maryland. Frankford Arsenal has since been phased out and Dr. Stuebing has been assigned to the Obscuration Sciences Section of the Chemical Systems Laboratory.

The use of trade names in this report does not constitute an official endorsement or approval of the use of such commercial hardware or software. This report may not be cited for purposes of advertisement.

TABLE OF CONTENTS

List of Figures

I. SURVEY OF ABSORPTION PHENOMENA IN THE NEAR INFRARED REGION

A. Attenuation of Electromagnetic Waves by a Dielectric Medium: A Simplified Dispersion Theory

We would like to describe, by the use of a simple model the absorption of electromagnetic radiation by non-conducting matter. We consider the material as consisting of a collection of N identical one-dimensional oscillators of mass m, charge e and elastic constant q, per unit volume. Free oscillations are described by

$$m\ddot{u} + m\bar{\omega}_o^2 u = 0 \qquad (1)$$

in which u is the displacement of the particle from its equilibrium position, m is the mass and $\bar{\omega}_o^2 = q/m$ is the resonant frequency. (The charge does not appear at this point.)

If the oscillator is coupled to a loss mechanism, a damping term must be added to the above equation to account for the energy loss. The resulting damped oscillator equation is

$$m\ddot{u} + m\gamma\dot{u} + m\omega_o^2 u = 0 \qquad (2)$$

in which γ is the damping constant.

The resonance frequency ω_o is different from $\bar{\omega}_o$. The interaction of the incident electromagnetic field with the oscillator is assumed to be as follows: The periodic electric field of the incident wave exerts a force on the damped oscillator and drives it at a frequency ω. We describe this motion with the forced oscillator equation

$$m\ddot{u} + m\gamma\dot{u} + m\omega_o^2 u = \text{Force} = eE_o e^{-i\omega t} \qquad (3)$$

where E_o is the maximum amplitude of the incident electromagnetic wave oscillating in the u direction at the site of the oscillator.

We can solve the above equation by substituting a trial solution of the form

$$u(t) = u_o e^{-i\omega t} \tag{4}$$

into equation (3). The result is

$$u(t) = \frac{eE_o/m}{\omega_o^2 - \omega^2 - i\gamma\omega} e^{-i\omega t} = \frac{e/m}{\omega_o^2 - \omega^2 - i\gamma\omega} E(t) \tag{5}$$

Thus, the amplitude u depends on the parameters of the oscillator $(e, m, \omega_o, \gamma,)$ as well as on the strength of the incident electromagnetic field.

So far we have considered just one microscopic process. The description of electromagnetic effects by Maxwell's equations uses macroscopic quantities and material constants such as the dielectric constant ε and permeability μ. The connection between the microscopic parameters of the oscillators and ε and μ is of interest here.

Since the amplitude u, derived above, is the displacement of one oscillator of mass m and charge e, eu is the induced dipole moment. The contribution of all N induced dipole moments per unit volume in the material is the polarization

$$P = Neu \tag{6}$$

Introducing u from equation (5) above gives

$$P = \frac{Ne^2}{m} \frac{1}{\omega_o^2 - \omega^2 - i\omega\gamma} E \tag{7}$$

It should be mentioned that in general E is a function of both, position (x) and time (t).

We now wish to solve the wave equation in the medium modelled by the damped oscillators. From equation (A-10) in appendix A, for a one-dimensional dielectric medium with no conductivity, the appropriate wave equation is

$$\frac{\partial^2 E}{\partial x^2} = \varepsilon_o \mu_o \frac{\partial^2 E}{\partial t^2} + \mu_o \frac{\partial^2 P}{\partial t^2} \tag{8}$$

where we have used the identity

$$\frac{1}{C^2} = \mu_o \varepsilon_o \tag{9}$$

The second term on the right hand side of equation (8) is called a source term. It accounts for the effect of polarization charges in the medium as discussed in appendix A. We now substitute for P and E in equation (8) displaying explicitly the spatial and temporal dependence of the electric field, i.e.

$$E(x,t) = E_o e^{\,i(Kx-\omega t)} \tag{10}$$

where $K = \frac{2\pi}{\lambda}$ is the magnitude of the wave vector. The result is

$$-K^2 = -\varepsilon_o \mu_o \omega^2 - \mu_o \frac{Ne^2}{(\omega_o^2 - \omega^2 - i\omega\gamma} \omega^2$$

or

$$\frac{K^2}{\omega^2} = \frac{1}{C^2}\left(1 + \frac{Ne^2/m\varepsilon_o}{\omega_o^2 - \omega^2 - i\omega\gamma}\right) \tag{11}$$

again using equation (9). We see that K^2 is complex. Since K is related to the index of refraction by $K = \frac{\omega}{C} n$, we introduce the complex index of refraction $n^*=n+ik$.
Then

$$\frac{K^{*2}}{\omega^2} = \frac{(n + ik)^2}{C^2} = \frac{n^2 - k^2 + 2ink}{C^2} \tag{12}$$

From equations (11) and (12) we obtain the real and imaginary parts of K^{*2} as

$$n^2 - k^2 = 1 + \frac{Ne^2 (\omega_o^2 - \omega^2)}{\varepsilon_o m [(\omega_o^2 - \omega^2)^2 + \omega^2\gamma^2]} \tag{13}$$

and

$$2nk = \frac{Ne^2}{\varepsilon_o m} \frac{\omega\gamma}{(\omega_o^2 - \omega^2)^2 + \omega^2\gamma^2} \tag{14}$$

We call n the refraction coefficient and k the extinction coefficient.

We have assumed above that the driving electrical field at the site of the oscillator is equal to the field of the electromagnetic wave outside of the material. This assumption implies that the density of oscillators in the material is low, somewhat as it would be in a gas. Conversely, for a dense distribution of oscillators we would have to add the influence of the surrounding material, the so-called Lorentz contribution. This latter case will not be considered here.

For such a low density medium the refractive index must be close to 1, the value in free space. As a consequence k is small compared to 1 and we have for n and k, using $\sqrt{1 + x} \simeq 1 + \frac{x}{2}$

$$n = 1 + \frac{Ne^2}{2\varepsilon_o m} \frac{(\omega_o^2 - \omega^2)}{(\omega_o^2 - \omega^2)^2 + \omega^2\gamma^2} \tag{15}$$

and

$$k = \frac{Ne^2}{2\varepsilon_o m} \frac{\omega\gamma}{(\omega_o^2 - \omega^2)^2 + \omega^2\gamma^2} \tag{16}$$

It is instructive to plot $n(\omega)$ and $k(\omega)$ and to consider three specific frequencies, $\omega = 0$, $\omega = \omega_o$ and $\omega = \infty$. To facilitate this discussion, we introduce the frequency-like term $\omega_p^2 = Ne^2/\varepsilon_o m$. Then equations (15) and (16) become respectively

$$n(\omega) = 1 + \frac{1}{2}\omega_p^2 \frac{\omega_o^2 - \omega^2}{(\omega_o^2 - \omega^2)^2 + \gamma^2\omega^2} \tag{17}$$

and

$$k(\omega) = \frac{1}{2}\,\omega_p^{\,2}\,\frac{\gamma\,\omega}{(\omega_o^{\,2} - \omega^2)^2 + \gamma^2\omega^2} \qquad (18)$$

Consider first the refractive index, $n(\omega)$ plotted in Figure 1.

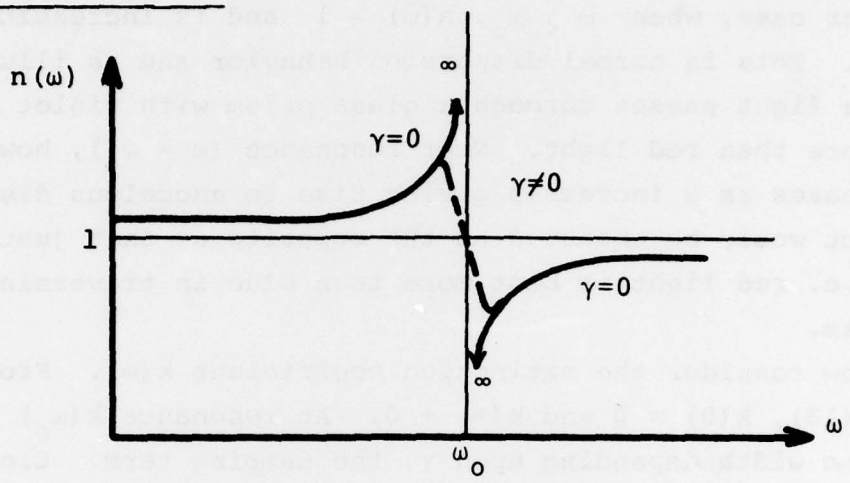

Fig. 1. Frequency dependence of refractive index for a dielectric described by a simplified dispersion model.

For $\omega = 0$, and $\gamma = 0$ (corresponding to a lossless medium, $n(0) = 1 + \frac{1}{2}(\omega_p/\omega_o)^2 = 1 + (Ne^2/2\varepsilon_o q)$. Numerically, $n(0)$ should correspond to expected static values for low density media, i.e., $n(0) \sim 1$. To see this, we choose reasonable values of N and q and evaluate $(\omega_p/\omega_o)^2$, i.e.,

$$\left(\frac{\omega_p}{\omega_o}\right)^2 \simeq \frac{(10^{30}\ \mathrm{m}^{-3})(1.6 \times 10^{-19}\ \mathrm{coul})^2}{(8.85 \times 10^{-12}\ \mathrm{farad\ m}^{-1})(10^{8}\ \mathrm{Nm}^{-1})} \simeq 3 \times 10^{-5}$$

Thus we see that $n(0) \simeq 1$ as expected. For $\omega \to \infty$, $n(\infty) \to 1$ which is the expected high frequency limit (for example, in the x-ray region). For $\omega = \omega_o$ (and $\gamma = 0$), $n(\omega)$ is singular. This situation is never realized for real systems, however, since some loss mechanism is always present. The effect of the non-zero damping term on $n(\omega)$ is shown as a dashed line in Figure 1. For this latter case, when $\omega \lesssim \omega_o$, $n(\omega) > 1$ and is increasing as ω increases. This is normal dispersion behavior and is illustrated when white light passes through a glass prism with violet light bending more than red light. Near resonance ($\omega = \omega_o$), however, $n(\omega)$ decreases as ω increases giving rise to anomalous dispersion. This effect would be observed as the opposite as that just described, i.e. red light is bent more than blue in traversing the glass prism.

We now consider the extinction coefficient $k(\omega)$. From equation (18), $k(0) = 0$ and $k(\infty) \to 0$. At resonance $k(\omega_o)$ has a maxima, the width depending upon γ, the damping term. Clearly for $\gamma = 0$, $k(\omega) = 0$ for all ω. $k(\omega)$ is plotted in Figure 2.

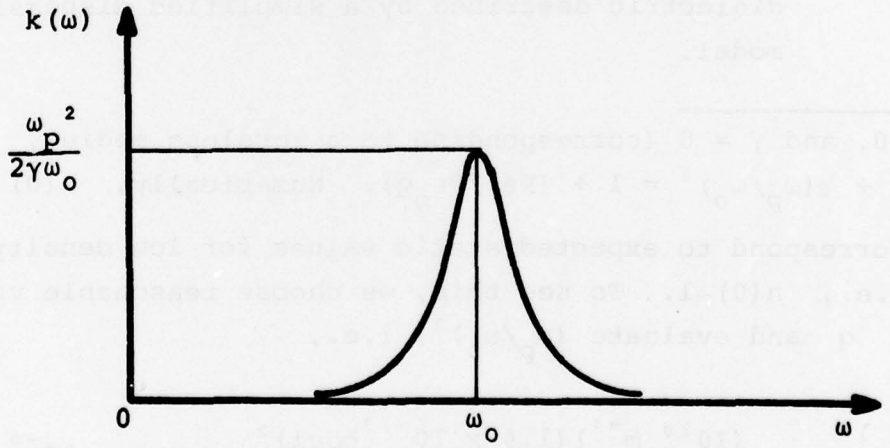

Fig. 2. Frequency dependence of extinction coefficient for a dielectric described by a simplified dispersion model.

It should be emphasized that the optical behavior just described was based upon a very elementary model composed of N identical oscillators. Real materials require more realistic models to accurately predict or describe observed measurements. As an example of a first attempt to extend the above model, we could relax the restriction of identical oscillators and assume that there are a certain fraction f_j of particles having resonant frequencies $\omega_{oj} = \sqrt{q_j/m}$. Then, for example, equation (11) becomes

$$K^{*2} = \frac{\omega^2}{C^2}\left[1 + \frac{Ne^2}{\epsilon_o m}\sum_j \frac{f_j}{(\omega_o^2 - \omega^2 - i\gamma_j\omega)}\right] \qquad (11')$$

with corresponding expressions for n^2-k^2 and $2nk$ following, as before.

Absorption Coefficient α

We now consider the effect of a complex wavenumber K^* on the propagation of a plane electromagnetic wave in a dielectric medium. Equation (10) is, using $K^* = \frac{\omega}{C}n^* = \frac{\omega}{C}(n+ik) = \frac{\omega}{C}n + i\frac{\omega}{C}k$

$$E(x,t) = E_o e^{i[\frac{\omega}{C}(n+ik)x-\omega t]}$$

$$= e^{-\frac{\omega}{C}kx} E_o e^{i(\frac{\omega}{C}nx-\omega t)} \qquad (19)$$

Since the intensity I of the radiation is the square of the electric field, we get

$$I = |E|^2 = EE^* = |E_o|^2 e^{-2(\frac{\omega}{C}k)x} \qquad (20)$$

Letting $I_o = |E_o|^2$ and

$$\bar{\alpha} = 2\alpha = 2\frac{\omega}{C}k \qquad (21)$$

we get Beer's Law

$$I(x) = I_o e^{-\bar{\alpha}x} \tag{22}$$

Thus $\bar{\alpha}$ tells us how much a layer of medium x units thick attenuates a beam of radiation of intensity I_o incident upon it. In particular, $\bar{\alpha}$, the absorption coefficient, measured in units of reciprocal centimeters, is such that in a distance $(\bar{\alpha})^{-1}$ the intensity falls from I_o to $I(= I_o/e)$. Experimentally $\bar{\alpha}$ is measured directly. (See discussion below.)

Using equation (21) and the well-known relations connecting the various wave parameters,

$$\omega = 2\pi f \ , \quad C = \lambda f \tag{23}$$

(C = speed of light in vacuo = 3×10^8 m/s; λ = wavelength of radiation) we see that

$$\alpha = \frac{2\pi}{\lambda} k$$

and

$$\bar{\alpha} = \frac{4\pi k}{\lambda} \tag{24}$$

$\bar{\alpha}$ is the quantity usually called the absorption coefficient. Equation (24) shows that $\bar{\alpha}$ is sufficient to determine the extinction coefficient k. Note that in entering a medium of refractive index n, a plane wave (1) slows down by a factor of $1/n$ (since $V = C/n$), (2) the wavelength decreases by a factor of $1/n$, ($\lambda_n = \lambda_o/n$; λ_o = free space wavelength), but (3) the frequency remains constant, that is

$$\omega = 2\pi f = 2\pi \frac{V}{\lambda_n} = 2\pi \frac{(C/n)}{(\lambda_o/n)} = \frac{2\pi C}{\lambda_o} = \omega \tag{25}$$

B. Attenuation of Electromagnetic Waves by a Conducting Medium

Let us compare a conducting medium with the dielectric medium previously considered. In a dielectric medium, the bound charges, represented as oscillators, form induced electric

dipole when exposed to incident electromagnetic wave. In a conductor, however, this polarization mechanism is missing since the electrons are not bound by a restoring force, but are considered to be almost free, except at the boundaries. The incident electromagnetic wave now does not produce oscillations of bound electrons, but does produce microscopic currents. We therefore expect, in the wave equation, a current density related term. From equation (A-10) of appendix A we obtain, for a one-dimensional conducting medium, a wave equation of the form

$$\frac{\partial^2 E}{\partial x^2} = \mu_o \varepsilon_o \frac{\partial^2 E}{\partial t^2} + \mu_o \frac{\partial j}{\partial t} \tag{26}$$

where j is the current density and is related to the velocity of the electrons by $j = Nev$ or to the applied instantaneous electric field by $j = \sigma E$, σ being the electrical conductivity. Again our objective is to correlate the conductors microscopic parameters with the measured optical "constants".

If we try to apply the damped oscillator equation (with no restoring force) we would have

$$m\ddot{u} + m\gamma\dot{u} = eE_o E^{-i\omega t} \tag{27}$$

The general solution of this equation is the sum of the solution of the homogeneous and inhomogeneous equations. For the homogeneous equation we have

$$m\ddot{u} + m\gamma\dot{u} = 0 \tag{28}$$

We try as a solution

$$u = e^{-\frac{t}{\tau}}$$

and obtain $\gamma = \frac{1}{\tau}$. The damping constant, γ, is inversely proportional to a decay time τ measured from an arbitrary zero point of time. This time is short (typically $\sim 10^{-13}$ sec) and we can neglect this contribution.

Considering the inhomogeneous equation, we observe that we could rewrite it as

$$\dot{mv} + m\gamma v = eE_o e^{-i\omega t} \tag{29}$$

since $\dot{u} = v$ and $\ddot{u} = \dot{v}$. This is advantageous since we would like to correlate $j = Nev$ to the microscopic process. A trial solution $v = v_o e^{-i\omega t}$ gives us

$$v = \frac{\frac{e}{m}}{-i\omega + \gamma} E \tag{30}$$

and for j we obtain

$$j = \frac{Ne^2}{m} \frac{1}{-i\omega + \gamma} \tag{31}$$

Considering that j now also depends on x as e^{iKx} we substitute for j from equation (31) and $E = E_o e^{i(Kx-\omega t)}$ into the wave equation (26), and obtain

$$-K^2 = -\mu_o \varepsilon_o \omega^2 + \mu_o \frac{Ne^2}{m} \frac{-i\omega}{-i\omega+\gamma}$$

or

$$K^2 = \frac{\omega^2}{C^2} \left[1 - \frac{Ne^2}{\varepsilon_o m} \frac{i}{i\omega-\gamma} \frac{i}{\omega}\right] \tag{32}$$

Let us again set $\frac{K^{*2}}{\omega^2} = \frac{(\bar{n} + i\bar{k})^2}{C^2}$ † which, when substituted into equation (32) and separated into real and imaginary parts, gives

$$\bar{n}^2 - \bar{k}^2 = 1 - \frac{Ne^2/\varepsilon_o m}{\omega^2 + \gamma^2} \tag{33}$$

---

†For the conducting medium, the optical parameters will be written as $\bar{n}$ and $\bar{k}$ to avoid confusion with the dielectric medium parameters.

and

$$2\,\bar{n}\,\bar{k} = \frac{Ne^2/\varepsilon_o m}{\omega^2 + \gamma^2}\,\frac{\gamma}{\omega} \qquad (34)$$

These expressions are different from the ones we previously obtained for the dielectric. For this case, there is no resonant frequency involved and, consequently, no singularity present when $\gamma=0$, except at $\omega=0$. For $\omega\to\infty$ we have $\bar{k}\to 0$ and $n\to 1$; which means, for example that x-rays can penetrate metals!

We again use the abbreviation $Ne^2/\varepsilon_o m = \omega_p^2$ and plot $\bar{n}$ and $\bar{k}$ as functions of ω. From equations (33) and (34) we see that for $\gamma\to 0$ and $\omega\to 0$, $\bar{n}^2-\bar{k}^2$ is negative and increasing, that is $|n| < |k|$ and $\bar{k}$ has large values, while for large ω we have $\bar{n}\simeq 1$ and $\bar{k}\simeq 0$. From equation (33) we obtain $\bar{n}=\bar{k}$ for $\omega=\omega_p$ if $\gamma\simeq 0$. From the equation for $2\bar{n}\bar{k}$ we conclude that $\bar{n}$ is smaller than 1. Therefore we have qualitatively for $\bar{n}$ and $\bar{k}$, the behavior sketched in Figure 3.

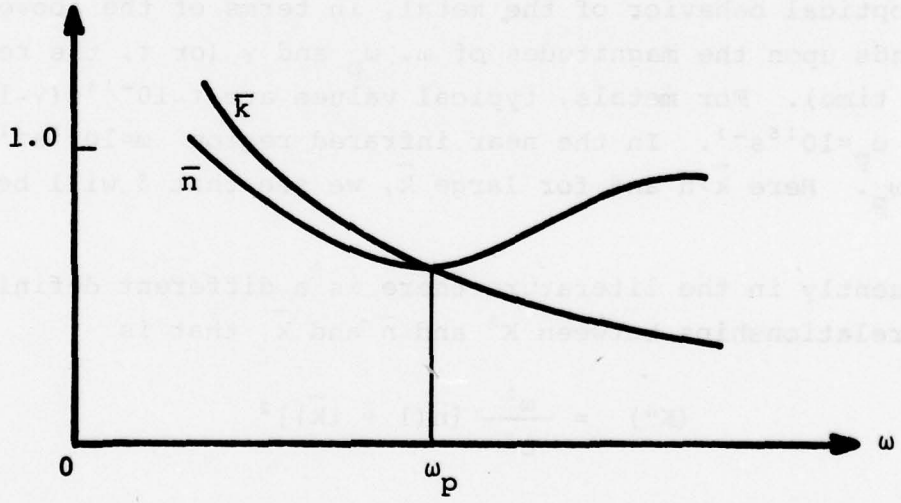

Fig. 3. Frequency dependence of refractive index $\bar{n}$ and extinction coefficient $\bar{k}$ for a metal.

The region where $\bar{k}$ becomes small and $\bar{n}$ approaches 1 is the region for which metals are transparent to electromagnetic waves. For large $\bar{k}$, metals are opaque and the metal reflects strongly. The wave can penetrate only a small distance into the metal before it is completely attenuated. An expression for the penetration depth is obtained by the introduction of $\bar{n}$ and $\bar{k}$ into the expression for the electromagnetic wave, equation (10), i.e.

$$E = E_o e^{i[\frac{\omega}{C}(\bar{n}+i\bar{k})x-\omega t]}$$

$$= E_o e^{-\bar{k}\frac{\omega}{C}x} e^{i[\frac{\omega}{C}\bar{n}x-\omega t]} \qquad (35)$$

Here $2\bar{k}\frac{\omega}{C}$ is the absorption coefficient $\bar{\alpha}$. The depth $x=\delta$ for which the wave is attenuated to e^{-1} of its incident value is called the skin depth and is obtained from $\frac{\omega}{C}\bar{k}\delta = 1$ or

$$\delta = \frac{C}{\bar{k}\omega} = \frac{1}{\alpha} \qquad (36)$$

The optical behavior of the metal, in terms of the above model, depends upon the magnitudes of ω, ω_p and γ (or τ, the relaxation time). For metals, typical values are $\tau \sim 10^{-13}s$ ($\gamma \sim 10^{13}s^{-1}$) and $\omega_p \simeq 10^{15}s^{-1}$. In the near infrared region $\omega \simeq 10^{13}s^{-1}$ so that $\gamma \simeq \omega < \omega_p$. Here $\bar{k} > \bar{n}$ and for large $\bar{k}$, we see that δ will be small.

Note

Frequently in the literature there is a different definition used for relationships between K^2 and $\bar{n}$ and $\bar{k}$, that is

$$(K^*) = \frac{\omega^2}{C^2}[\bar{n}(1 + i\bar{k})]^2$$

$$= \frac{\omega^2}{C^2}[\bar{n}^2(1 - \bar{k}^2) + 2i\,\bar{n}\,\bar{k}] \qquad (37)$$

For the real and imaginary part we would then have

$$n^2(1 - \bar{k}^2) = 1 - \frac{\omega_p^2}{\omega^2 + \gamma^2} \tag{38}$$

and

$$2\bar{n}\,\bar{k} = \frac{\omega_p^2}{\omega^2 + \gamma^2}\,\frac{\gamma}{\omega} \tag{39}$$

C. Absorption of Electromagnetic Waves by Molecules

1. Normal Vibrations

In considering the dynamics of a molecule composed of N atoms, 3N coordinates are required to describe its translational, rotational and vibrational motion. If we exclude linear and diatomic molecules from our consideration, 3 coordinates are used each for the description of the translatory and rotatory motion of the entire molecule. The remaining 3N-6 coordinates describe the vibrational motion of the molecule, that is we have 3N-6 vibrational degrees of freedom. (Linear and diatomic molecules have only 3N-5.) For the determination of the vibrational frequencies it is necessary to know the kinetic as well as the potential energy of the atom in the molecular system. In the Born-Oppenheimer approximation, one considers the electrons, which are contributing to the bonding in the molecule, to move much faster than the nuclei (with or without attached core electrons). The bonding electrons are responsible for the potential energy of the force field in which the nuclei are undergoing their vibrations.

The coordinates used for the description of the vibrational problem may be initially of various kinds such as cartesian coordinates or internal coordinates. The kinetic and potential energy is expressed in these coordinates.

The potential energy V is expressed as a Taylor series about the equilibrium position of the molecule

$$V = V_o + \sum_{i=1}^{3N-6} \left(\frac{\partial V}{\partial q_i}\right)_o q_i + \frac{1}{2} \sum_{i,j=1}^{3N-6} \left(\frac{\partial^2 V}{\partial q_i \partial q_i}\right)_o q_i q_j \qquad (40)$$

$$+ \text{(higher order terms)}$$

where the q_i's are the mass weighted coordinates of the various point masses (nuclei with and without core electrons). In the harmonic oscillator approximation, terms higher than second order are neglected. Since $(\partial V/\partial q_i)_o$ is, by definition of the equilibrium position, equal to zero, and V_o is a scale factor (constant), the potential energy becomes a quadratic expression in $q_i q_j$, i.e.

$$2V = \sum_{i,j=1}^{3N-6} k_{ij}\, q_i\, q_j \qquad (41)$$

where the k_{ij}'s are the force constants. Using these coordinates, the kinetic energy is expressed as

$$2T = \sum_{i=1}^{3N-6} \dot{q}_i^{\,2} \qquad (42)$$

Then, Lagrange's formalism yields the equations of motion

$$\ddot{q}_j + \sum_{i=1}^{3N-6} k_{ij}\, q_i = 0 \qquad j = 1, 2, \ldots, 3N-6 \qquad (43)$$

A solution of this eigenvalue problem, that is a solution of the system of linear second order differential equations, is obtained by introducing a trial solution into the above equations:

$$q_i = A_i \cos(\omega t + \phi) \qquad (44)$$

Here $\omega=2\pi f$ where f is the vibrational frequency to be determined, and ϕ is a phase factor. The systems of differential equations yield a set of simultaneous, homogeneous linear algebraic equations in the 3N-6 coordinates.

$$\sum_{i=1}^{3N-6} (k_{ij} - \delta_{ij}\omega^2)\, A_i = 0 \qquad j = 1 \ldots\ldots 3N-6 \qquad (45)$$

This system of equations can be solved only if the secular determinant vanishes, i.e.

$$\begin{vmatrix} k_{11}-\omega^2 & \cdots & k_{12} & \cdots & k_{1,3N-6} \\ \vdots & & k_{22}-\omega^2 & & \vdots \\ \vdots & & & & \vdots \\ \vdots & & & & \vdots \\ k_{3N-6,1} & \cdots & k_{3N-6,2} & \cdots & k_{3N-6,3N-6}-\omega^2 \end{vmatrix} = 0 \qquad (46)$$

Solution of the polynomial of order 3N-6 will yield at most 3N-6 different ω^2's. It may be possible that some of the ω^2's are the same. In such a case, the associated vibrational frequencies are said to be degenerate. For each of the 3N-6 values of ω we will obtain a set of A_{ik}'s from the system of algebraic equations. These sets of A_{ik}'s are called eigenvectors. We can use the 3N-6 eigenvectors to compose a transformation matrix L of the form

$$L = \begin{pmatrix} A_{11} & & A_{1,3N-6} \\ \vdots & & \vdots \\ \vdots & & \vdots \\ \vdots & & \vdots \\ A_{3N-6,1} & & A_{3N-6,3N-6} \end{pmatrix} \qquad (47)$$

This matrix transforms the original coordinate system into the normal coordinate system.

$$\begin{pmatrix} Q_1 \\ \cdot \\ \cdot \\ \cdot \\ \cdot \\ \cdot \\ Q_{3N-6} \end{pmatrix} = L^{-1} \begin{pmatrix} q_1 \\ \cdot \\ \cdot \\ \cdot \\ \cdot \\ \cdot \\ q_{3N-6} \end{pmatrix} \tag{48}$$

The importance of this transformation can best be seen if we go back to the expression for the kinetic and potential energy. Both are transformed by the above matrix from their dependence on the q_i into dependence on Q_i , i.e.

$$2T = \sum_{i=1}^{3N-6} \dot{q}_i^{\,2} \xrightarrow{L} \sum_{i=1}^{3N-6} \dot{Q}_i^{\,2}$$

$$2V = \sum_{i,j}^{3N-6} k_{ij} q_i q_j \xrightarrow{L} \sum_{i=1}^{3N-6} \tilde{k}_i Q_i^{\,2} \tag{49}$$

where the $\tilde{k}_i$ are combinations of the k_{ij} . The equation of motion appears in normal coordinates as

$$\ddot{Q}_i + \tilde{k}_i Q_i = 0 \tag{50}$$

that is, the different equations are no longer coupled to one another and, therefore, each coordinate is associated solely with one vibrational mode of the molecule. In normal modes all the atoms vibrate in phase, that is, they all pass through their equilibrium positions at the same time.

The application of quantum mechanics to the system of N atoms does not change the results drastically. The Schroedinger equation is solved in terms of normal coordi-

nates. The modes of the molecular motion are associated with wave functions and eigenvalues. The classical vibrational frequency is the same as the one obtained from quantum mechanics. However, selection rules are introduced and, consequently, the absorption intensity is modified.

2. Selection Rules for a Vibrating Molecule

A vibrating molecule may absorb a light quantum hf, where f corresponds to the energy difference between the initial and exited (finite) state. The Bohr frequency condition is

$$f = \frac{E_f - E_i}{h} \tag{51}$$

where h = Planck's constant. The selection rules are obtained by expanding the electric dipole moment μ of the molecule in terms of normal coordinates, i.e.

$$\mu = \mu_o + \sum_{K=1}^{3N-6} \left(\frac{\partial \mu}{\partial Q_K}\right)_o Q_K + \text{(higher order terms)} \tag{52}$$

Again, in the harmonic oscillator approximation, the higher order terms are neglected for the dipole moment matrix element $\int \psi_i \mu \psi_f d\tau$. We then have

$$\int \psi_i \mu_o \psi_f d\tau + \sum_{K=1}^{3N-6} \left(\frac{\partial \mu}{\partial Q_K}\right) \int \psi_i Q_K \psi_f d\tau. \tag{53}$$

ψ_i may be written as a product of the initial states of all vibrations $\psi_i = \prod_{K=1}^{3N-6} \psi_{oK}$ and, if only the j^{th} state is singly exited, ψ_f may be written as

$$\psi_f = \psi_{1j} \prod_{K \neq j}^{3N-6} \psi_{oK} \tag{54}$$

Introduction of the wave function into the expression for the matrix element of the dipole moment yields

$$\int \left(\prod_{K}^{3N-6} \psi_{oK} \right) \mu_o \left(\prod_{K \neq j}^{3N-6} \psi_{oK} \right) \psi_{1j} \, d\tau + \sum_{K=1}^{3N-6} \left(\frac{\partial \mu}{\partial Q_K} \right)_o \int \left(\prod_{K}^{3N-6} \psi_{oK} \right) Q_K \left(\prod_{K \neq j}^{3N-6} \psi_{oK} \right) \psi_{1j} \, d\tau \qquad (55)$$

The first integral vanishes since μ_o is a constant and $\int \psi_{oj} \, \psi_{ij} \, d\tau = 0$ from the orthogonality condition. In the second integral all terms in the sum of the type $\int \psi_{oK} \, Q_K \, \psi_{oK}$ are zero by symmetry. The only non-zero term is

$$\left(\frac{\partial \mu}{\partial Q_j} \right)_o \int \psi_{oj} \, Q_j \, \psi_{1j} \, d\tau \qquad (56)$$

This term would be zero if $\left(\frac{\partial \mu}{\partial Q_j} \right)_o$ would vanish or if we would not have initially chosen only one vibration to be singly excited.

The general selection rule for harmonic oscillator vibrational transition is

$$\Delta j = \pm 1 \qquad (57)$$

The permanent dipole moment has no influence on the vibrational transition, but the change in the dipole moment with respect to the vibrational coordinate (Q_K) is important and must be non-zero. The harmonic oscillator approximation is sufficient to explain the most intense transitions. By considering the influence of the higher order terms in equations (40) and (55) on the dipole moment μ, weaker, previously-forbidden, transitions may be predicted.

3. The Concept of Group Frequencies

Reviewing the near infrared absorption spectra of a large number of chemical compounds, one observes that absorption bands at certain frequencies are related to the occurence of certain molecular groups in the molecule. For example, the bands around the 3000 cm^{-1} region are related to C-H stretching vibrations. A careful study of this phenomenon has revealed that the relationship between observed bands and molecular groups is almost unique and therefore one speaks of the fingerprint region if the analytical aspect of the near infrared region is considered. The correspondence between normal vibrations and group frequencies is, for most of the cases, simple. Let us consider the normal mode of a certain frequency which is also listed as group frequency. The atoms belonging to the group frequency vibrations are undergoing large amplitude vibrations in the normal mode compared to all the other atoms. From the point of view of interaction with the electromagnetic field the effect of all the other atoms may be neglected.

D. Lattice Vibrations in Dielectric Media

1. Bulk Material

The periodic arrangement of molecules in a crystal lattice leads to new types of absorption phenomena which are observed in addition to the absorption due to the internal vibrations. For most molecules in crystal form, lattice vibration absorption is observed in the middle and far-infrared regions. Only for small molecules may we observe this type of absorption in the near infrared. Consequently, the one dimensional linear chain may well serve as a model for the discussion of this phenomena. In this model, the unit cell contains two atoms with different effective charges so that a contracting force exists between an atom and its nearest

neighbors. One can see immediately the occurrence of two fundamental modes, one in which the two atoms of the unit cell move in opposite directions and one in which they move in the same direction. The former is called the longitudinal optical mode, with frequency ω_T , whereas the latter is the longitudinal acoustical mode, with zero frequency. A more detailed analysis leads to the dispersion relation of the modes, that is, the relationship between the frequency and wave vector for all possible modes in the Brillouin zone.

If we extend these considerations to three dimensions, we find that there are two transvers optical and two transverse acoustical mode branches possible, in addition to the longitudinal one. Of all these modes, we are only interested in those which lead to strong optical absorption. For interactions with an electromagnetic field to occur, we need, as usual, a component of the electric field in the direction of the change of the dipole moment of the chain. Since the transverse modes are degenerate, we have only two branches of modes to consider. Selection rules predict that frequencies belonging to zero wave vectors are the fundamental frequencies. Difference and summation frequencies may occur at other non-zero wave vectors with far lesser intensity. The fundamental frequencies can easily be visualized by considering the chain as composed of two sublattices of equal atoms having sublattices oscillating rigidly against one another. This results in a large change in the dipole moment and, consequently, in a large absorption. The absorption corresponding to this fundamental vibration is called, in ionic crystals, the reststrahlen band. The names relate to the fact that in very strong absorption, the incident wave is attenuated in such a small surface layer that the surface reflects most of the radiation, as is found for a metal.

Theoretically derived quantitative expressions for the absorption coefficient are difficult to obtain since it is necessary to know the wave functions of the ground and excited state in order to calculate the change in the dipole moment. Experimentally, one proceeds as discussed at the beginning of this section, and determines k, from which α can be obtained.

2. Dielectric Powders

We have just seen that the fundamental absorption process in ionic type crystals involves the transverse optical mode. In special cases, it may also involve the longitudinal optical mode. If the diameter of the crystal becomes very small, the frequency of the fundamental vibration shifts to higher values. It has been observed, e.g. in MgO micro-crystals of radius 50A to 800A, that the lattice absorption peak shifts up by 10 cm^{-1}. The reason for this shift can be seen by considering the number of atoms on the surface of the crystals (having neighbors partially surrounding them) compared to the number of atoms in the interior of the crystal (having neighbors completely surrounding them). For a particle radius of 50A, about 25% of the ions are on the surface, whereas for a radius of 380A there are only 3% on the surface. Since the shift is to higher frequencies with decreasing size, one may conclude that the lattice spacing on the surface is smaller. This may indeed be proven. As a consequence of this finding, one expects a strong influence on the lattice vibrational frequency of the surrounding matrix due to the polarization charges. One finds, however, a different frequency ω_F which is related to the transverse optical mode frequency by

$$\omega_F^2 = \frac{\varepsilon_o + 2\varepsilon_m}{\varepsilon_\infty + 2\varepsilon_m} \omega_T^2 \qquad (58)$$

where ε_0 and ε_∞ are the low and high frequency dielectric constants and ε_m the dielectric constant of the surrounding medium. The frequency shift due to this effect can be remarkable. In $BaTiO_4$, for example, the lattice vibrational frequency of the bulk material is at 33 cm^{-1}, whereas for small spheres in powder form in a surrounding medium with $\varepsilon_m = 1$, one observes a value of 400 cm^{-1}.

Experiments on small particles are hampered by the scattering effects of the particles. Quantitative experimental values can be obtained via the dielectric constant and from that, the determination of α may be made.

E. Absorption of Electromagnetic Waves by Semiconductors

For absorption by semiconductors in the near infrared spectral region we consider: (a) Transitions of electrons across the band gap, (b) free carrier absorption and interband absorption, and (c) multiphonon absorption.

1. Band Gap Absorption

The strongest absorption in the near infrared is due to the transition of electrons from the valence band to the conduction band. These transitions are only possible if the energy of the absorbed photon is comparable or larger than the band gap energy, that is $hf \geq E_g$. For photons with hf smaller than E_g these transitions are not possible. A plot of the absorption coefficient $\alpha(f)$ against the photon energy shows therefore a strong increase of absorption near $hf=E_g$; this is called the band edge absorption. For $hf < E_g$ the material is relatively transparent. The absorption in the $hf > E_g$ region is relatively strong; α has values of the order of 10^4/cm.

The transition from the valence to the conduction band can be a "direct" or an"indirect"transition, depending on the structure of the bands. The energy difference E_g

between the bands depends in general on the crystal structure. Direct transitions occur if the minimum of the conduction band and the maximum of the valence band both are situated at the same $\vec{K}$ value (e.g. at $\vec{K} = 0$). The electron then makes a "vertical transition" without change in momentum ($\vec{K}$ is conserved) and the energy difference is $E_g = hf$. An indirect transition occurs if the minimum of the conduction band and the maximum of the valence band are not situated at the same point in $\vec{K}$ space. In order to conserve momentum a phonon is either absorbed or emitted. Since the photon momentum is small in the energy region under consideration, the phonon makes up for the change in $\vec{K}$. On the other hand, the phonon energy is small compared to the energy of the absorbed photon so that $hf \simeq E_g$. The absorption probability for an indirect process is smaller that that for a direct process.

(a) Absorption coefficient for direct transitions

Let us assume a parabolic relationship between E and K at the maximum of the valence band and at the minimum of the conduction band where the direct transition occurs. The absorption coefficient is then found to be:

$$\alpha(f) = A\sqrt{(hf - E_g)} \tag{59}$$

where

$$A = \frac{q^2 \left(2\,\frac{m_h^* m_e^*}{m_h^* + m_e^*}\right)^{3/2}}{n\,C\,h^2\,m_e^*} \tag{60}$$

q is the charge of the electron, m_h^* and m_e^* are the effective masses of holes and electrons respectively, n is the real refractive index, C is the speed of light, and h is Planck's constant. For $n = 4$ and $m_h^* = m_e^* = m_e$,

where m_e is the free electron rest mass, we have

$$\alpha(f) = 2 \times 10^4 \, (hf - E_g)^{\frac{1}{2}} \tag{61}$$

$\alpha(f)$ is given in cm^{-1} if h and E_g are inserted in units of electron volts.

(b) Absorption coefficient for forbidden direct transitions

Sometimes direct transitions are forbidden by selection rules for $\vec{K} = 0$ (symmetry), but allowed for $\vec{K} \neq 0$. For this case the absorption coefficient is found to be:

$$\alpha(f) = A' \, (hf - E_g)^{3/2} \tag{62}$$

where

$$A' = \frac{4}{3} \, \frac{q^2 \, \dfrac{m_h^* m_e^*}{m_h^* + m_e^*}}{n \, C \, h^2 \, m_e^* \, m_h^*(hf)} \tag{63}$$

and for the case discussed above [paragraph (a)] we have

$$\alpha(f) = 1.3 \times 10^4 \, \frac{(hf - E_g)^{3/2}}{hf} \, , \; cm^{-1} \tag{64}$$

again, hf and E_g are in ev's.

(c) Absorption coefficient for indirect transitions

The indirect transitions are two-step processes and, consequently, the interaction of photons with electrons and phonons have to be considered. The absorption coefficient has been shown to be

$$\alpha(f) = A\left\{\left[\frac{(hf - E_g - E_p)^2}{-1 + \exp(-E_p/kT)}\right] + \left[\frac{(hf - E_g + E_p)^2}{1 - \exp(-E_p/kT)}\right]\right\} \tag{65}$$

where E_p is the energy of the phonon. The first term is due to a process with phonon absorption, the second with phonon emission. The constant A has a complicated appearance. In many cases it is determined by an experimental fit to the data.

2. Free Carrier Absorption

Free carrier absorption is of importance in semiconductors as it is in conductors. Absorption due to free carriers may be observed in the near and far infrared. The absorption of photons by the electrons in the periodic field of the crystal is strictly not allowed as a consequence of conservation of momentum. However, a perturbation involving lattice vibrations (phonons) relaxes the restrictions and absorption of photons is possible. The absorption coefficient may be calculated on the basis of classical theory by assuming an oscillating electron without a restoring force and using an effective mass m_e^* in place of the electron rest mass m_e. One obtains:

$$n^2 - k^2 - \varepsilon = \frac{Nq^2/m_e^*\varepsilon_o}{\omega^2 + \gamma^2} \tag{66}$$

$$2nk\omega = - \frac{Nq^2/m_e^*\varepsilon_o}{\omega^2 + \gamma^2} \tag{67}$$

where $\gamma = \frac{1}{\tau}$ and τ is the collision time. For wavelengths up to a few hundred micrometers, the absorption coefficient may be expressed as:

$$\alpha(f) = \frac{\lambda^2 q^3}{4\pi^2 C^3 n\, \varepsilon_o} \left(\frac{Nq}{m_e^2 \mu_e} \right) \tag{68}$$

where λ is the wavelength; q is the electron charge; m_e is the electron mass; μ_e is the electron mobility; C is the speed of light; n is the refractive index and ε_o is the static dielectric constant. The order of magnitude of the absorption coefficient $\alpha(f)$ is 10 - 100 cm^{-1} for free carrier absorption in, for example, n-type InAs in the 3-15μm region. This value is two orders of magnitude smaller than that for band edge absorption. Interband absorption and absorption due to holes results in absorption coefficients of the same magnitude.

3. Multiple Phonon Absorption

The absorption due to lattice vibrations occurs, for most material, in the middle and far infrared. For ionic crystals these lattice vibrations show up as reststrahlen bands. These bands are due to fundamental modes of the lattice with $\vec{K} = 0$, $\vec{K}$ being the crystal momentum vector. Multiple phonon absorption of the summation type can be observed in the near infrared region. Absorption due to such processes are relatively weak, because these processes are second order effects. They appear as modulation on top of the free carrier absorption.

F. Absorption of Electromagnetic Waves by Metals

1. Bulk Materials

The dependence of the optical constants on the microscopic parameters of bulk conducting materials has been discussed in the first chapter on "simplified dispersion theory". In this simple approach the plasma frequency and relaxation time are the characteristic parameters for the absorption process. This process is similar to the absorption in semiconductors as we have just seen in section I. E.2 "free carrier absorption".

2. Metal Powders

By considering metal powder instead of the bulk material one anticipates changes analogous to those observed for dielectric bulk material and their powders. The important parameter is the plasma frequency and for particles of about 10A diameter, a broadening of the plasma resonance peak is observed. Theoretically, this broadening is described by a decreased electron mean free path due to scattering at the particle surface. This macroscopic explanation has been more successful than considerations from a quantum mechanical point of view. In thin conducting films, on the other hand, one has observed effects which are interpreted as the breakdown of the continuous conduction band into discreate states by reducing the thickness of the film from bulk material dimensions. The evaluation of the absorption coefficient from experimental measurements proceeds as outlined before.

G. Absorption of Electromagnetic Waves by One-Dimensional Conductors

Recently a number of linear conducting materials have been developed. These polymeric materials have metallic behavior in the direction of the chain and almost insulator-like properties in the direction perpendicular to the chain. An example of a polymeric one-dimensional conductor (not recognized as such initially) is the H-sheet polarizer invented by E. Land in 1938. This polarizer is made of polyvinyl alcohol chains which are aligned by uniaxial stretching of the material. The sheet is impregnated with iodine by immersing it into a special ink. The iodine atoms or molecular clusters are believed to donate electrons. These electrons constitute the free charge carriers involved in the conduction process as in a metallic conductor. Incident light with its electric field vector oriented parallel to the polymer chain is absorbed so that the sheet acts as a polarizer.

As a result of the considerable interest in linear conductors, a number of one-dimensional linear polymeric conductors have been extensively studied, e.g. $(SN)_x$ and polyacetylene-iodide. These materials are black and light-weight, and for polyacetylene-iodide, the absorption in the near infrared region is broad and strong, but without distinctive absorption features. A quantitative absorption study is underway in our laboratory.

II. QUANTITATIVE ANALYSIS OF ABSORBING MATERIALS

An electromagnetic wave incident upon a material will interact with it, and have its energy changed, by three types of mechanisms: (1) Reflection, in which a fraction of the incident radiation is deflected backwards; (2) scattering, in which a fraction of the incident radiation is scattered in all directions (characteristics depend upon relationship between particle size and wavelength of radiation, optical inhomogeneities, etc.); and (3) absorption, the general term describing the conversion of radiant energy into thermal energy. Generally, all these processes are present to varying degrees and, are sensitive to the wavelength of the incident radiation. We are interested here in the absorption process and assume that the beam incident normally upon, and entering the medium, has a radiant power I_o. Upon passing through a uniform layer b units thick, the radiant power is attenuated to a value $I(b)$ given by the absorption (Lambert-Bouguer) law

$$I(b) = I_o e^{-\alpha(\nu)b} \tag{69}$$

The product $\alpha(\nu)b$ is the optical density or absorbance and $\alpha(\nu)$ is the (frequency-dependent; $\nu = \frac{1}{\lambda}$) absorption coefficient. As mentioned in paragraph I. A, $\alpha(\nu)$ is related to the imaginary part of the complex index of refraction $k(\nu) = Im[n(\nu)^*]$ by

$$\alpha(\nu) = \frac{4\pi}{\lambda} k(\nu) = 4\pi\nu k(\nu) \tag{70}$$

The extinction coefficient $k(\nu)$ is a function of frequency [as is $n(\nu)$]. Equations (69) and (70) show that, in principle, one has only to measure the total sample thickness b and $\frac{I(b)}{I_0}$ to extract values of $\alpha(\nu)$ and, if desired $k(\nu)$, for materials in the form of uniform slabs. If the material of interest is dissolved in a suitable (i.e., non-absorbing, non-interacting, etc.) solvent, Eqn. (69)is written as

$$I(b) = I_0 e^{-\varepsilon(\nu)cb} \tag{71}$$

usually referred to as Beer's Law. Here b is the optical path length through the solution of concentration c moles/liter characterized by a molar extinction coefficient $\varepsilon(\nu)$ measured in units of liter/mole-cm. Clearly for a liquid film confined to a cell of thickness b cm, comparison of equations (69), (70) and (71) gives

$$\varepsilon(\nu) = \frac{4\pi}{c}\nu k(\nu) \tag{72}$$

The concentration may be obtained from

$$c = \frac{\rho}{M}\phi \tag{73}$$

where ρ is the solute density (in gm/mℓ), M is the molecular mass (in gm/mole), and ϕ is volume fraction of solute [i.e., mℓ (solute)/liter (solution)]. Clearly, in assuming Beer's Law to hold for a solution, we must determine experimentally the absorbance A and either $\varepsilon(\nu)$ or c. In routine analysis of materials, $\varepsilon(\nu)$ is usually known and the concentration c is the desired quantity.

A quantity of considerable interest, especially as related to the study of molecular dynamics, is the integrated absorption intensity, defined here as

$$A = \int_{\nu_1}^{\nu_2} \alpha(\nu)d\nu \tag{74}$$

Here ν_1 and ν_2 are frequencies (wave numbers) sufficiently far removed from the band center that $\alpha(\nu_1) = \alpha(\nu_2) \simeq 0$.

Theories relating the microscopic processes to $\alpha(\nu)$ are mathematically quite involved. The resonance absorption of a molecule in the gaseous state, for example, depends on both the vibrational frequency, and the frequency of the overall rotation of the molecule. Interactions between the vibrational and rotational motion occur. The analysis, theoretical or empirical, should reveal the observed frequencies. The intensities may then be calculated by assuming, for example, a Boltzmann equilibrium distribution of the oscillators. The effect of the collisions between the molecules, that is, line broadening, might be considered as well as other factors affecting the microscopic processes, and therefore the absorption coefficient. Calculations are only possible for the simplest of molecules. For larger molecules one needs interaction constants of the vibration-rotation interaction or the vibrational wave functions of the ground and first excited state. These are difficult to calculate and empirically not easy to determine. As an "over-simplified" rule, however, in most cases the absorption coefficient is proportional to the resonance frequency and the square of the matrix element of the dipole moment. In liquids, the overall rotation of the molecule is suppressed and the collisions between molecules play a more dominant role. The absorption process might be considered as consisting of resonance absorption and orientational absorption. The former is an absorption centered about the vibrational resonance frequency where the rotational states do not exist as individual levels, but contribute to a broad absorption band. The latter depends on the orientation (and reorientation) of permanent dipoles in an applied electromagnetic field (Debye absorption). An empirical description of these two processes is of the form

$$\alpha(t) = a_1 e^{-t/\tau} \cos(\omega t + \phi) + a_2 e^{-t/\tau}$$

If the constants a_1, τ, a_2 and ϕ are determined, $\alpha(\nu)$ may be obtained through a Fourier transformation. Here τ is a characteristic relaxation time associated with the orientation. Theoretical calculations of $\alpha(\nu)$ using procedures from statistical mechanics, as well as quantum mechanics, are difficult and lengthy. However, this is a very active field since one can deduce the correlation function and obtain an estimate of the molecular behavior subsequent to an assumed initial configuration. The time interval considered is of the order of 10^{-11}-10^{-12} sec.

Experimental Methods

The use of the Lambert-Bouguer-Beer Law appears deceptively straightforward. While the method is not sophisticated, there are certain precautions that must be considered so that the data yield true material parameters rather than experimental artifacts. We will consider in limited detail, the more significant of these features.

A. Liquids

1. Deviations from Beer's Law and Photometric Error

The attenuation of a beam of light as it passes through a specimen depends upon the samples thickness b, its absorption coefficient α and the particular wavelength λ or frequency (actually wavenumber $\nu = \lambda^{-1}$). Ultimately, the attenuation depends upon the number of absorbing particles (molecules) "seen" by the optical beam. Provided that the number of particles and the volume containing them remain constant, the absorption coefficient $\alpha(\nu)$ suffices to characterize the substance. Such is the case for solids and pure liquids. For solutions or mixtures of liquids, however, this condition is not fulfilled and it becomes necessary to relate the absorption to the sample concentration. (The analogous situation for gases would require that the effect of pressure be considered.) This is done in the case of Beer's Law, since the absorbance is given by

$$A = \varepsilon(\nu)\ c\ b \tag{75}$$

For a substance to "obey" Beer's Law then, the absorbance must be proportional to the concentration. Unfortunately, this is not always found and deviations, both real, as in the case of refractive index changes due to high solute concentrations, and apparent, due to instrumental limitations and non-symmetrical chemical equilibrium, are encountered. The real deviations arise when the measured absorption is no longer the sum of the absorptions for all separate particles. More specifically the relation

$$A = \sum_{i=1}^{N} A_i = b \sum_{i=1}^{N} \varepsilon_i(\nu) c_i \tag{76}$$

where i labels the species and N is the total number of species present, is <u>not</u> obeyed. This non-ideal behavior is a result of formation of molecular aggregates or clusters by solute-solute and solute-solvent interactions. This type of deviation may be used to study molecular interactions, and is therefore, not without some value.

The experimental deviations arise because Beer's Law is rigorously correct only for monochromatic radiation. The finite slit width of the instrument monochromator allows a band of frequencies to be detected so that the magnitude of the deviation depends on the ratio of the slit width to the absorption band width observed. This effect has no compensating benefits, but must be tolerated. However, empirical determination of factors affecting the absorbance may still be evaluated provided the aforementioned instrumental factors are maintained constant.

The above considerations of deviations leads to some practical rules-of-thumb for choosing the experimental parameters. To eliminate clustering effects in solutions, concentrations below about .01M should be used. However, the instruments ability to detect small changes in radiant power

limits the dilution to about 10^{-7}M. Concommitant with the desire for low concentrations is the instrument's need for sufficient energy at the detector so that photometric error may be minimized. Here again a suitable balance must be sought since for a low solute concentration, a weak absorption band results and the instrument "sees" a small difference between incident and transmitted power, and thus a relatively large error in absorbance. Alternatively, for a more concentrated solution, the absorption band is strong and insufficient power reaches the detector, also giving inaccurate results. An appropriate intermediate range of absorbance can be obtained starting with Eqn. (75) rewritten as

$$\varepsilon(\nu) = \frac{A}{bc} = \frac{1}{bc} \log \frac{1}{T} = - \frac{1}{bc} \log T \qquad (77)$$

Here we have used the identity A = -log T, where T is transmission, usually associated with I/I_0. Our aim is to minimize the error in the molar extinction coefficient $\varepsilon(\nu)$ by minimizing the error in T. The fractional error in $\varepsilon(\nu)$ is

$$\frac{d\varepsilon(\nu)}{\varepsilon(\nu)} = - \frac{\log e}{\varepsilon(\nu)bc} \frac{dT}{T} \qquad (78)$$

where log means $\log_{10}$ ("ℓn" is reserved for $\log_e$) log e = 1/2.30 = .434, and dT is the uncertainty in T. To minimize $d\varepsilon/\varepsilon$, differentiate Eqn. (78) and equate the result to zero. The result gives log T + log e = 0, log T = -.434, or T_{opt} = .368 for the optimum value of transmission to minimize instrument photometric error.

To summarize, optimum accuracy in the determination of $\varepsilon(\nu)$ is obtained when the solute concentration is such that (1) molecular clustering is avoided and (2) the transmission is in the range of 30-40% for absorption band minima.

2. Cell Losses

In stating the Lambert-Bouguer-Beer Law [Eqns. (69) and (71)] the quantity I_o is taken as the incident beam power and I the transmitted power. Since a beam of light is partially reflected at the interfaces between two dielectric media, the incident power arriving at the first surface of a liquid cell is not totally transmitted to the second surface, where additional reflection also takes place. In fact, multiple reflections will take place at all four interfaces of a liquid cell consisting of two (assumed) flat windows separated by an (assumed) uniform space. Ignoring the convergence of the optical beam in the sample compartment of most infrared spectrometers, the fraction of incident radiation reflected at normal incidence can be calculated from

$$\frac{I_{refl}}{I_o} = \left(\frac{n_2 - n_1}{n_2 + n_1}\right)^2 \qquad (79)$$

For an NaCl window ($n_2 = 1.54$) in air ($n_1 = 1.00$), $I_{refl}/I_o = .045$ or 4.5% of the incident power is reflected from the first surface. Clearly, for accurate quantitative work, the various cell losses must be accounted for. One method suggested by Draegert, et al [J.O.S.A. 56, 64,(1966)] and used in this reported work is to consider the actual incident beam to be represented by $r_o I_o$ and the transmitted beam by rI. The coefficients r and r_o, accounting for the cell losses, need not be equal.

The measured transmission of the cell-solution system is $T_m = rI/r_o I_o$ while the true transmission is $T = e^{-\varepsilon(\nu)bc} = I/I_o$. Equation (71) now becomes

$$\ell n T_m = \ell n \left(\frac{r}{r_o}\right) - \varepsilon(\nu)cb \qquad (80)$$

If one makes a series of measurements of T_m for various cell thicknesses b, holding the concentration c constant and plots $\ell n\ T_m$ vs b, the resulting curve is a straight line whose slope is $-\varepsilon(\nu)c$. The molar extinction coefficient $\varepsilon(\nu)$ can then be extracted from the data by, viz. a least squares fit. The ordinate intercept of this curve gives r/r_o, but is of little practical significance. As indicated above, we have used this method to obtain $\varepsilon(\nu)$ for tri-n-butyl phosphate. As a check on the validity of the method, we determined the molar extinction coefficient $\varepsilon(\nu)$ and from it, the extinction coefficient $k(\nu) = (c/4\pi)\ \varepsilon(\nu)/\nu$ [see Eqn. (72)] for pure, spectral quality chloroform ($CHCl_3$). Our results at 3020 cm^{-1} (3.31μ) [k(3020) = 0.011] agree very well with those reported by Hauranek and Jones [Spectrochim. Acta 32A, 111 (1976)] [k(3020) = 0.0115] using a considerably more involved procedure.

3. Other Corrections

Using detailed computer calculations for measured and simulated data, Jones and coworkers* have considered factors contributing to spectrophotometric errors in determining the optical constants of materials confined to thin cells (1-100μ). For information only, we list these factors with our parenthetical comments where appropriate.

(a) Construction of precision (thin) cells.
(b) Distortion caused by interference and reflection within the cell and at cell surfaces.
(c) Polarization discrimination of monochromator.
(d) Distortion caused by wedge-shaped cell, i.e., non-parallel windows.

---

* See Spectrochima Acta 32A, 75-123 (1976)

(e) Non-normal beam incidence due to beam convergence - (effects interference fringe pattern when $b \gtrsim 100\mu$).

(f) Surface roughness of window faces - negligible in mid and far-infrared, i.e. for $\lambda \geq 2.5\mu$ (cell windows should be demounted and repolished ~ every three months).

(g) Indeterminacy in cell thickness value caused by cold flowing of window material and (e) (cell spacing should be measured before and after spectrum is obtained).

(h) Dispersion distortion of absorbing solutes in non-absorbing solvents [important for high concentrations (i.e. c ~ 50 mol%) in thin cells (i.e. $b \sim 1\mu$)].

(i) Various computational errors generated, for example, by truncation of wave number interval in computer program (not a factor in this work).

Many of the above-listed factors are of significant importance only if extremely accurate (i.e. archival) determinations of optical constants are sought. In these cases considerable experimental control and computer time are required.

B. Solid Films

1. Reflection Losses

Since free standing solid films have only two interfaces, as compared to four in a liquid film cell, the optical problems involved are somewhat simpler. Reflections will still occur at the first and second surfaces and interference fringes may appear if the film thickness has the appropriate value. Fringes may be eliminated by (a) casting a film directly on a transparent window or (b) coating the film with Nujol (mineral oil) and pressing it against a

thick window [Latinski, C., Anal. Chem. 30, 2071 (1958)]. Of course if the film is thick enough, the fringe separation is less than the monochromator resolution, and interference fringes are not observed.

Reflection losses at the air/film interfaces may be treated in a manner similar to that described above for liquid film measurements. That is, the spectrum is scanned repeatedly using films of varying thickness. One then uses the equation

$$\ell n\ T_m = \ell n\left(\frac{r}{r_o}\right) - \alpha(\nu)\, b \qquad (81)$$

to extract the absorption coefficient $\alpha(\nu)$. The extinction coefficient $k(\nu) = Im[n^*(\nu)]$ may then be obtained [see Eqn. (70)], if so desired.

2. Other Errors

The discussion presented above in paragraphs A.2 and A.3 are generally applicable for thin, free-standing films, with some minor modifications possibly required. Therefore, they will not be further addressed here. Of greater importance here are two experimental difficulties related to sample preparation. First: Is the (solid) sample available in thin film form? Here "thin" means sufficiently transparent in the wavelength region of interest so that photometric errors (see paragraph A.1) are minimized, i.e. so that $T \simeq 30\text{-}40\%$. Second: Is the thin film of uniform thickness?

If the solid material is insoluble, such as with some polymers, films may be produced by rolling or pressing the bulk sample in a molten state. Both methods offer positive and negative features, For example, hot pressing of polymer beads on powder may not offer sufficient temperature control,

allowing for thermal degradation, or may allow air pockets or bubbles to form within the film, causing photometric inaccuracies. Rolling samples may avoid these problems, but introduces orientation effects, possibly undesirable. Sectioning thin slices is possible if a microtome is available and if the material is rigid enough.

For soluble materials, casting films from solutions is a practical method. Numerous techniques have been developed to produce uniformly thick films, many of which have been reviewed by Mano and Durao [J. Chem. Ed., 50, 228 (1973)]. The choice of solvent, environment of cast solution and condition of the substrate surface are among the relevant factors to be considered here.

III. EXPERIMENTAL RESULTS

A. Polymethylmethacrylate (PMMA)

PMMA samples were obtained from cast sheets of Lucite supplied by the Plastic Products and Resins Department of E. I. DuPont de Nemours & Co. Lucite pieces were dissolved in reagent grade toluene. The resultant solution was poured into teflon casting dishes which were set upon a leveled microflat. The rate of solvent evaporation was controlled by enclosing the casting dishes within a large glass container (inverted fish tank). Sample thickness was controlled by varying the volume of solution into the casting dish.

In spite of the above precautions undertaken to obtain uniform films, the resulting sample thicknesses exhibited considerable variation. The three PMMA films used to determine $\alpha(\nu)$ were measured and found to have the following values.

$$b = \begin{cases} 0.375 \pm .029 \text{ mil} = 9.53 & 0.74\mu m \ (\ 8\%) \\ 0.225 \pm .050 \text{ mil} = 5.72 & 1.27\mu m \ (22\%) \\ 0.169 \pm .067 \text{ mil} = 4.29 & 1.70\mu m \ (40\%) \end{cases}$$

Film thickness was measured with a Starrett Gauge (No. 25-209). The average of b "seen by" the optical beam is listed above together with the (%) deviation. This magnitude of the deviation in film thickness is the principal source of error in the determination of $\alpha(\nu)$ for PMMA and is a consequence of the need to have films thin enough so that sufficient radiant energy is transmitted and reaches the detector of the spectrophotometer (see paragraph II). Since strongly absorbing materials are of primary interest in this project, the problems associated with producing "uniform and thin" films cannot be avoided.

The infrared spectra of the three films of PMMA were recorded from 4000 to 800 cm^{-1} (2.5 - 12.5μm). The value of $\alpha(\nu)$ was calculated from Eqn.(81) at 20 cm^{-1} intervals from 4000 to 2000 cm^{-1} (2.5 - 5μm) and at 10 cm^{-1} intervals from 2000 to 850 cm^{-1} (5.50 - 12.5μm) All values reported were calculated by a linear regression analysis on the data points (ℓn T vs b). The results are presented in Fig. 4a and 4b.

B. Tri-n-Butyl Phosphate

Solutions of tri-n-butyl phosphate (TBP) were prepared by mixing purified-grade solute with spectral quality solvents (CCl_4 and CS_2). Various concentrations were produced by measuring known quantities of TBP, using Van Slyke pipets, into calibrated volumetric flasks and filling to level with solvent. Calibrated, sealed liquid cells were used for path lengths down to approximately 0.1 mm. At higher concentrations, demountable cells, using various thinner spacers, were required. Where possible, path lengths were determined by measuring cell fringe spacing. For very thin cells, for which the fringe method is not applicable, the spacer thick-

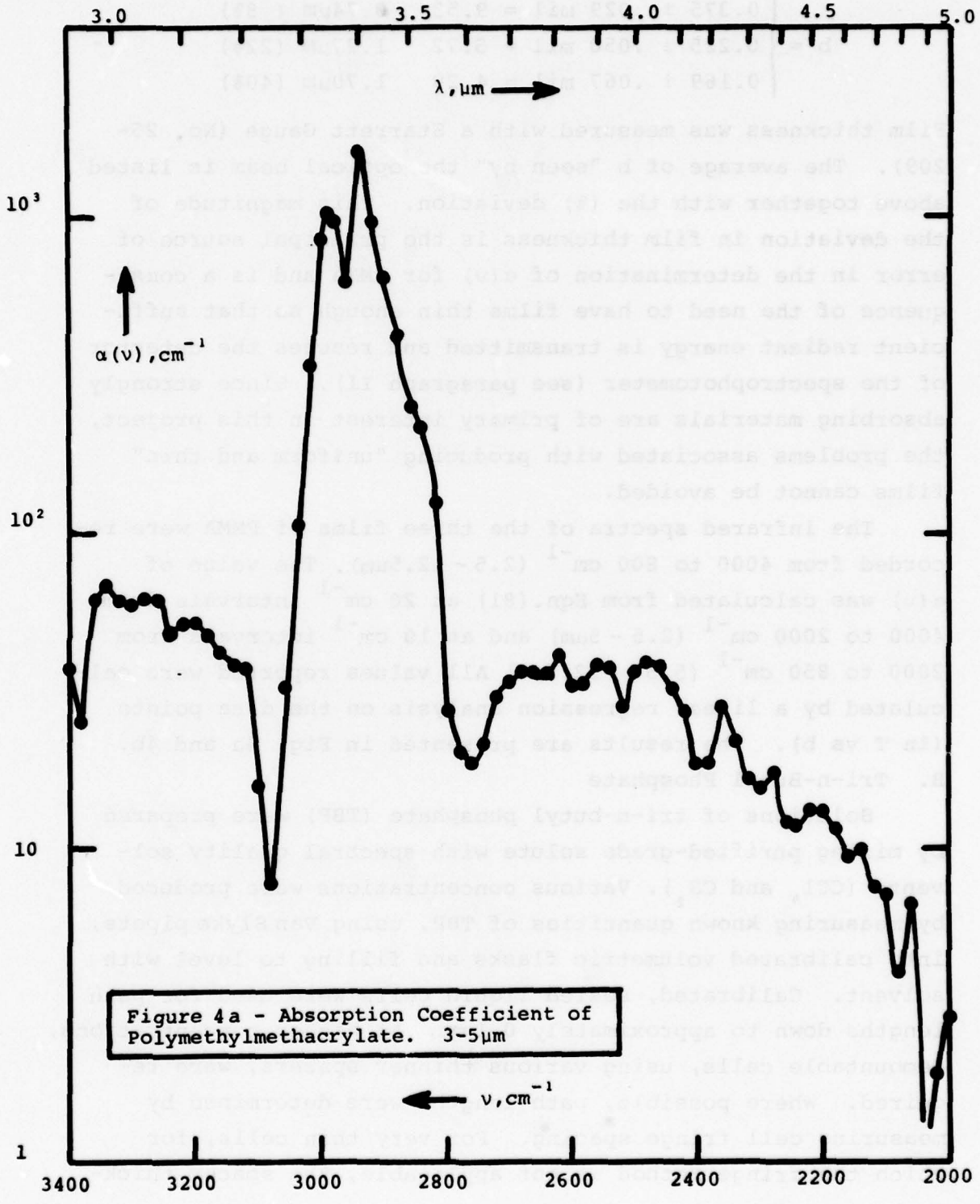

Figure 4a - Absorption Coefficient of Polymethylmethacrylate. 3-5μm

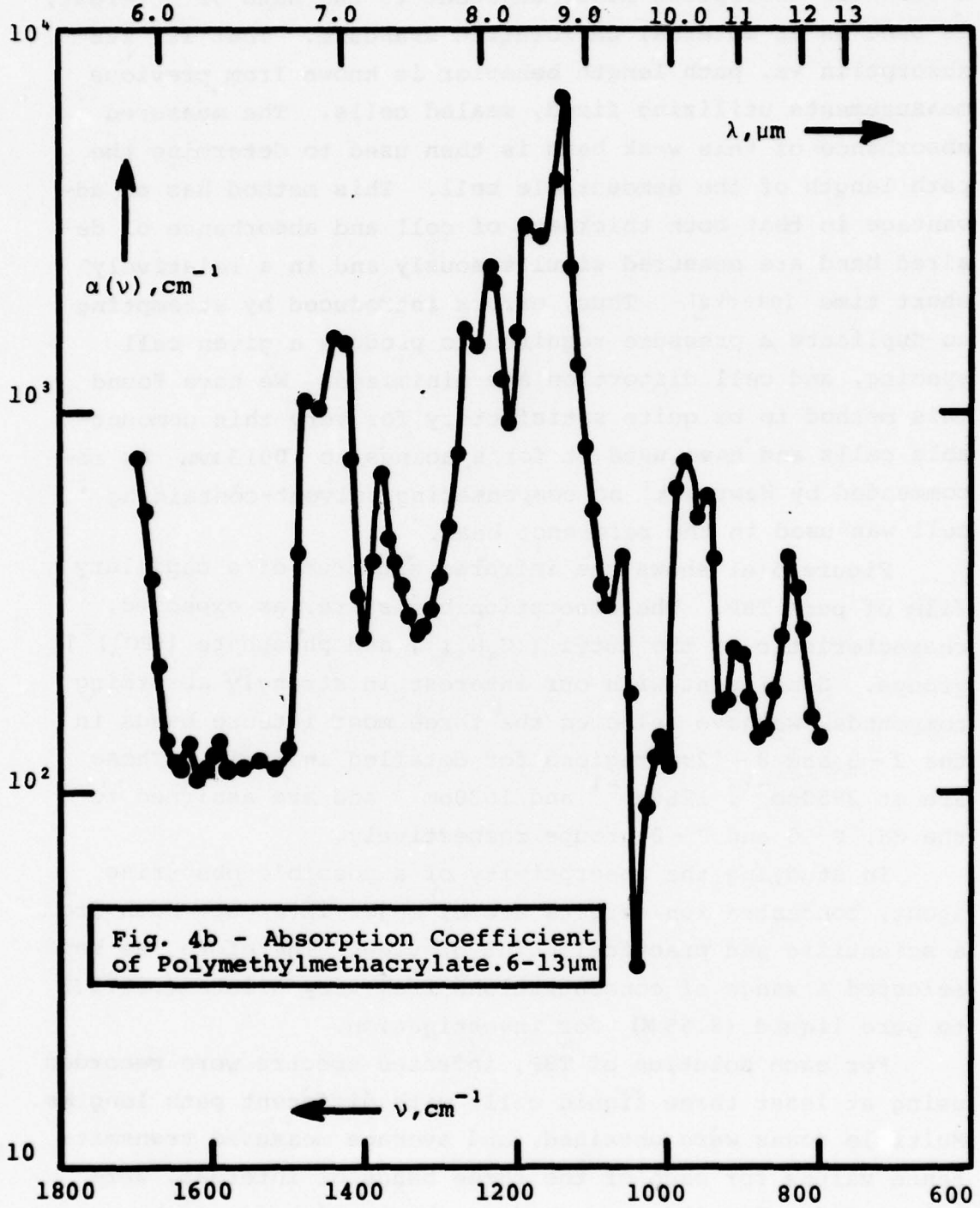

Fig. 4b - Absorption Coefficient of Polymethylmethacrylate.6-13μm

ness was determined as follows. For a given concentration, a weak TBP absorption band, adjacent to the band of interest, is used as an internal calibration standard. That is, its absorption vs. path length behavior is known from previous measurements utilizing fixed, sealed cells. The measured absorbance of this weak band is then used to determine the path length of the demountable cell. This method has an advantage in that both thickness of cell and absorbance of desired band are measured simultaneously and in a relatively short time interval. Thus, errors introduced by attempting to duplicate a pressure required to produce a given cell spacing, and cell distortion are minimized. We have found this method to be quite satisfactory for very thin demountable cells and have used it for spacings to .0013 mm. As recommended by Hawranek[1] no compensating solvent-containing cell was used in the reference beam.

Figure 5(a) shows the infrared spectrum of a capillary film of pure TBP. The absorption bands are, as expected, characteristic of the butyl [$(C_4H_9)^+$] and phosphate [$(PO_4)^{\equiv}$] groups. Consistent with our interest in strongly absorbing compounds, we have selected the three most intense bands in the 2 - 5 and 8 - 12μm regions for detailed analysis. These are at 2950cm^{-1}, 1280cm^{-1} and 1030cm^{-1} and are assigned to the CH, P = 0 and P - 0 groups respectively.

In studying the absorptivity of a possible obscuring agent, concentration effects are of major interest, both from a scientific and practical point of view. Therefore, we have selected a range of concentrations from very dilute (.0073 M) to pure liquid (3.65 M) for investigation.

For each solution of TBP, infrared spectra were recorded using at least three liquid cells with different path lengths. Multiple scans were obtained, and average measured transmittance values for each of the three bands of interest, were calculated. Eqn.(80) was used to obtain $\varepsilon(\nu)$ for each con-

[1] [Spectrochimia Acta 32A, 75 (1976)]

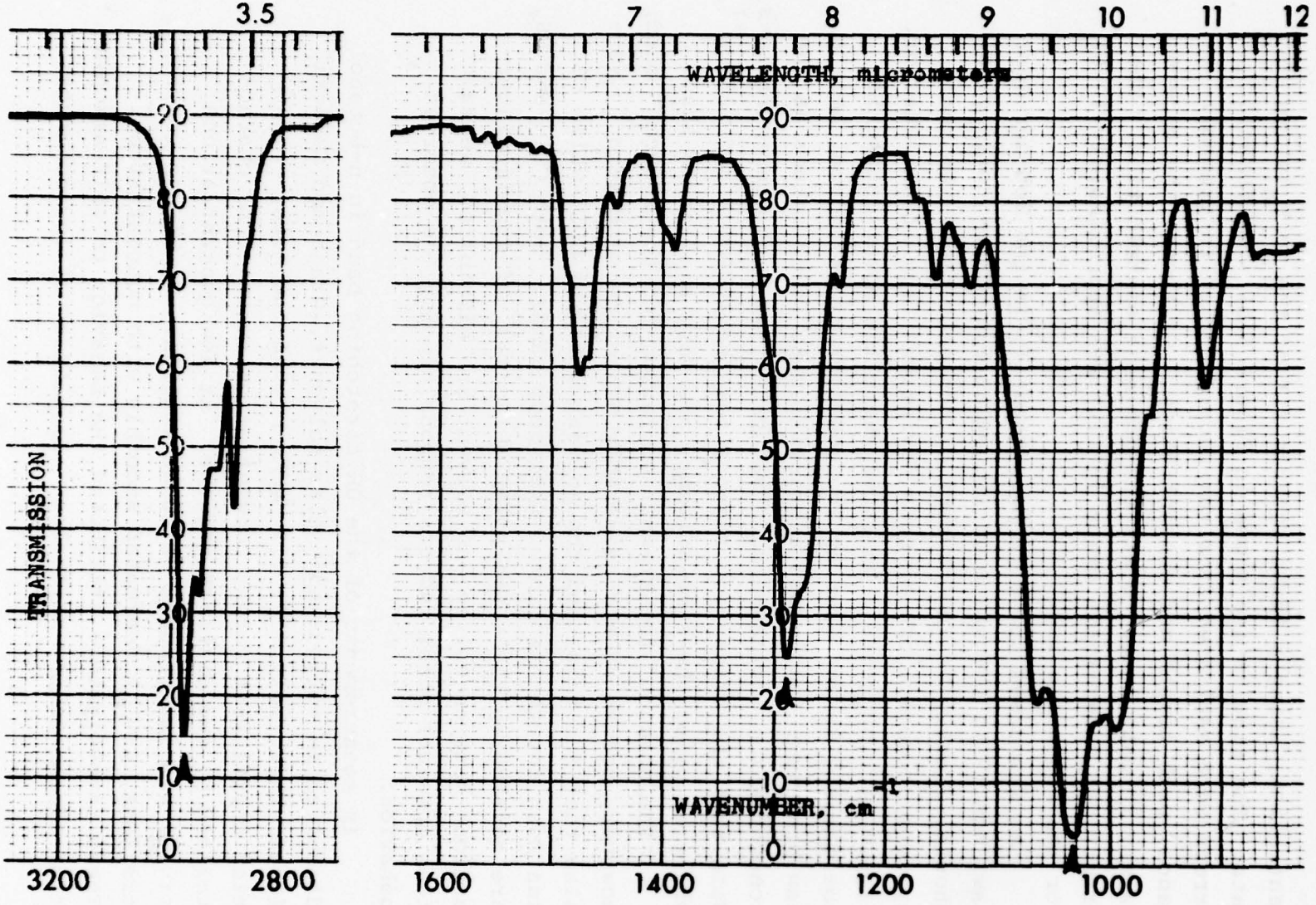

Fig. 5a - Infrared Spectrum of a Capillary Film of Tri-n-Butyl Phosphate. (Bands used for analysis are indicated.)

centration, using a least squares fit of the $\ell n\ T_M(\nu)$ vs. b data. The results are shown in Figure 5(b). Systematic errors were estimated from the uncertainties in transmittance, path length and concentration. Of these, the uncertainty in path length b was the dominant contribution. The fractional determinate error in $\varepsilon(\nu)$ was approximately 4 - 6% for the bands studied.

As discussed above in paragraph II, in the Bouguer-Beer law, Eqn.(71), the value of the molar extinction coefficient should, ideally be independent of concentration. In real systems, however, one expects deviations from ideal behavior. Figure 5(b) suggests a behavior where the molar extinction coefficient is constant at low concentrations (normal Beer's law behavior), undergoes a transition to lower values as the concentration increases and "saturates" at high concentrations. Note that the transition regions for the $1030cm^{-1}$ and $1280cm^{-1}$, obtained using the same solvent, are very similar in shape.

The onset of the transition region for the $2950cm^{-1}$ band, however, occurs at a considerably higher concentration. Note also that for this band the solvent used was CCl_4 while CS_2 was used for the two lower frequency bands. Both CCl_4 and CS_2 are considered to be non-polar solvents. If dipolar interactions between solute and solvent are eliminated, we must then consider other factors responsible for the observed behavior.

In measurements of the OH stretching band in n-butanol dissolved in various non-polar solvents, Graja and Malecki [Chem. Phys. Lett. 34, 373 (1975)] found the molar extinction coefficient versus concentration curve to be characterized by two distinct regions. At low concentrations $\varepsilon(\nu_{OH})$ was independent of concentration. At higher concentrations, $\varepsilon(\nu_{OH})$ decreased smoothly with concentration. These investigators attributed the behavior to self-association of the solute molecules. In effect, at low concentra-

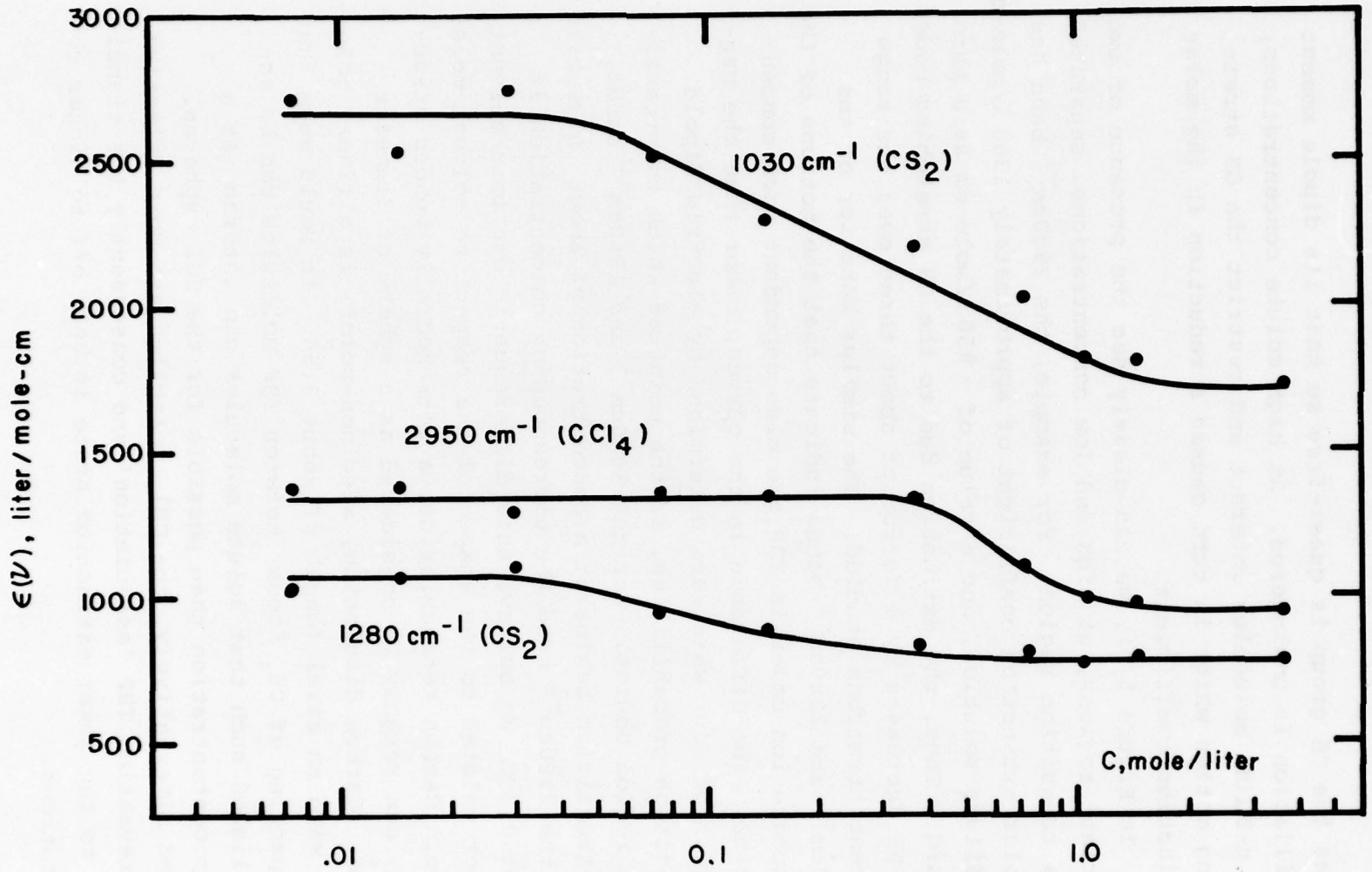

Fig. 5b - Concentration-Dependence of the Molar Extinction Coefficient for the Three Strongest Infrared Absorption Bands in Tri-n-Butyl Phosphate.

tions the OH group is quasi-free so that its dipole moment oscillation is unhindered. At high solute concentrations, the n-Bu OH molecules interact and restrict the OH stretching motion which in turn causes a reduction in the molar extinction coefficient.

In Figure 5(b), we can clearly see the presence of two distinct regions, at high and low concentrations, separated by a transition region. For example, the $2950cm^{-1}$ band has a molar extinction coefficient of approximately 1365 ℓ/mole-cm in dilute solution, and a value of ~ 950 ℓ/mole-cm as a pure liquid. Thus, the extinction due to the CH stretching modes in TBP decreases by a factor of about three over the range of concentrations studied. The similar behavior of the $1030cm^{-1}$ and $1280cm^{-1}$ bands indicate that the motions of the phosphate ion modes in TBP are also dependent upon concentration. The difference in the curves, other than the magnitudes of $\varepsilon(\nu)$ which are determined by electric dipole transition probabilities, is the point at which the transition region begins. For the $1030cm^{-1}$ and $1280cm^{-1}$ bands, the transition begins at a concentration of about .03 M while for the $2950cm^{-1}$ band the corresponding concentration is about 0.3 M. We believe this difference is due to a solvent effect related to the shapes of the respective solvent molecules. Carbon tetrachloride, a tetrahedrally bonded structure, can roughly be considered as a sphere of diameter ~3.6Å. Carbon disulphide, also non-polar, is a linear molecule with an axial length of about 3.6Å. It would seem that the packing of CS_2 "rods" between TBP molecules can be accomplished such that solute molecules can interact at a lower concentration than possible for the CCl_4 spheres. Viewed alternatively, the CCl_4 molecules are more effective at preventing TBP 'association' and consequently the transition to the lower extinction state is held off to higher concentrations.

The solvent effects described here are manifest in the experimental procedure to determine the material parameter, $\varepsilon(\nu)$. As such they have limited applicability to possible field use of TBP as an obscurant. However, the fact that the extinction coefficient is concentration-dependent is of interest. In particular, these results show that it can be erroneous to evaluate the molar extinction coefficient by extrapolating the curves of $\varepsilon(\nu)$ versus concentration to dilute conditions. Also, in the case of TBP, 'more is not better'.

C. Cellulose

Samples of regenerated cellulose film were obtained from the Film and Packaging Division of FMC Corporation. Two film thicknesses were specially prepared for our use and contained no plasticizer. The films were dried under tension in FMC Corporation's Laboratory. While the moisture content of cellulose is very sensitive to atmosphere humidity, we were unable to determine any appreciable difference between the spectrum of a film stored in air and one which had been dryed for 24 hours under vacuum. No additional drying at elevated temperatures was attempted by us.

Cellulose is a naturally occurring material having a typical fibre structure. It is the main component of the cell walls of most plants and, thus, has been estimated to comprise about 33% of all vegetable matter. Cellulose, together with starch and glycogen are polysaccharides composed of glucose only. The glucose units are linked by β-glycoside bonds resulting in a repeat or monomer unit represented by

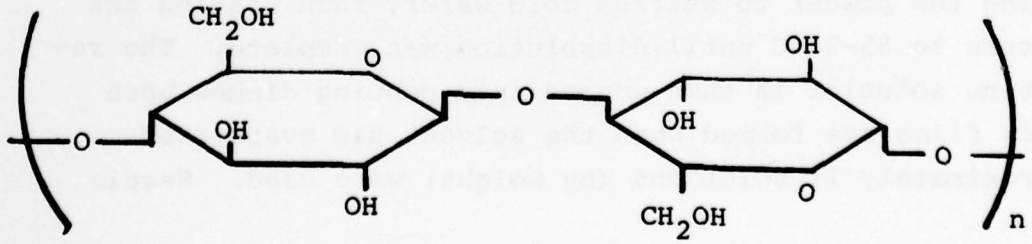

and referred to as a cellobiose unit.

Industrial cellulose, as used here, is extracted from wood pulp by a straight-forward, but carefully controlled process. Our laboratory is not equipped to perform the extraction procedure. The films kindly prepared for us by FMC Corporation were received with average thicknesses of 0.45 mil. (.0011 cm) and 0.95 mil. (.0024 cm). Normally, such optical path lengths for transmission measurements are suitable for determining absorption coefficients. However, cellulose is highly absorbing in the 3600-3000 cm^{-1} (2.8-3.33μ) and 1200-950 cm^{-1} (8.3-10.5μ) regions. This is, of course, a highly desirable property in terms of the goals of the overall project. The low transmission of the samples in these regions made quantitative measurements impractical. Therefore, in Figs. 6 a and 6 b, where the behavior of $\alpha(\nu)$ for cellulose is presented, those regions for which numerical values are not reported are indicated by dashed lines. It may be possible to produce samples of cellulose that are thin enough to yield transmissions of 30% in those highly absorbing regions, yet are mechanically stable enough to be treated as free films. However, to do so should require a special order to FMC Corporation without additionally imposing on their generosity and cooperation.

D. Polyvinyl Alcohol

Polyvinyl alcohol (PVA) resin, in powdered form, was donated by American Hoechst Corp. Material received was designated as Moviol 4-88 and characterized by a viscosity of 4 cP (centipoise), for a 4% aqueous solution at 20°C, and an 88% degree of hydrolysis. PVA solutions were produced by adding the powder to stirred cold water, then heating the mixture to 85-90°C until dissolution was complete. The resulting solution is then poured into casting dishes upon which films are formed when the solvent has evaporated. Approximately 1% solutions (by weight) were used. Sample

thickness was controlled by varying the volume of solution poured into the casting dish.

Three films were produced with thicknesses of 23.6±2.5μm, 3.81±0.00μm, and 2.90±0.61μm. The errors in the thicknesses were determined by measuring only the variations of those areas of the films "seen" by the optical beam of the instrument. The optical density of the 23.6μm film was too large to allow for quantitative results to be reported over the wavelength ranges of interest. Therefore, values of $\alpha(\nu)$ reported in Fig. 7 a and b represent data obtained from the two thinner films.

E. Ureaformaldehyde

Powdered ureaformaldehyde (UF) resin was supplied by R. W. Doherty (CSL-Edgewood Arsenal) and characterized as having an approximate particle size of 4μm diameter. The resin is crosslinked* and so is not soluble. Because of its relatively poor characterization, ureaformaldehyde could only be investigated as a powder suspended in a matrix (Nujol Oil). Quantitative measurement techniques for such powders are presently being developed in our laboratory. Consequently, only a qualitative spectrum of UF is presented (see Fig. (8a and 8b) at this time.

*Personal communication with J. Schwendeman, Monsanto Corp. Dayton, Ohio

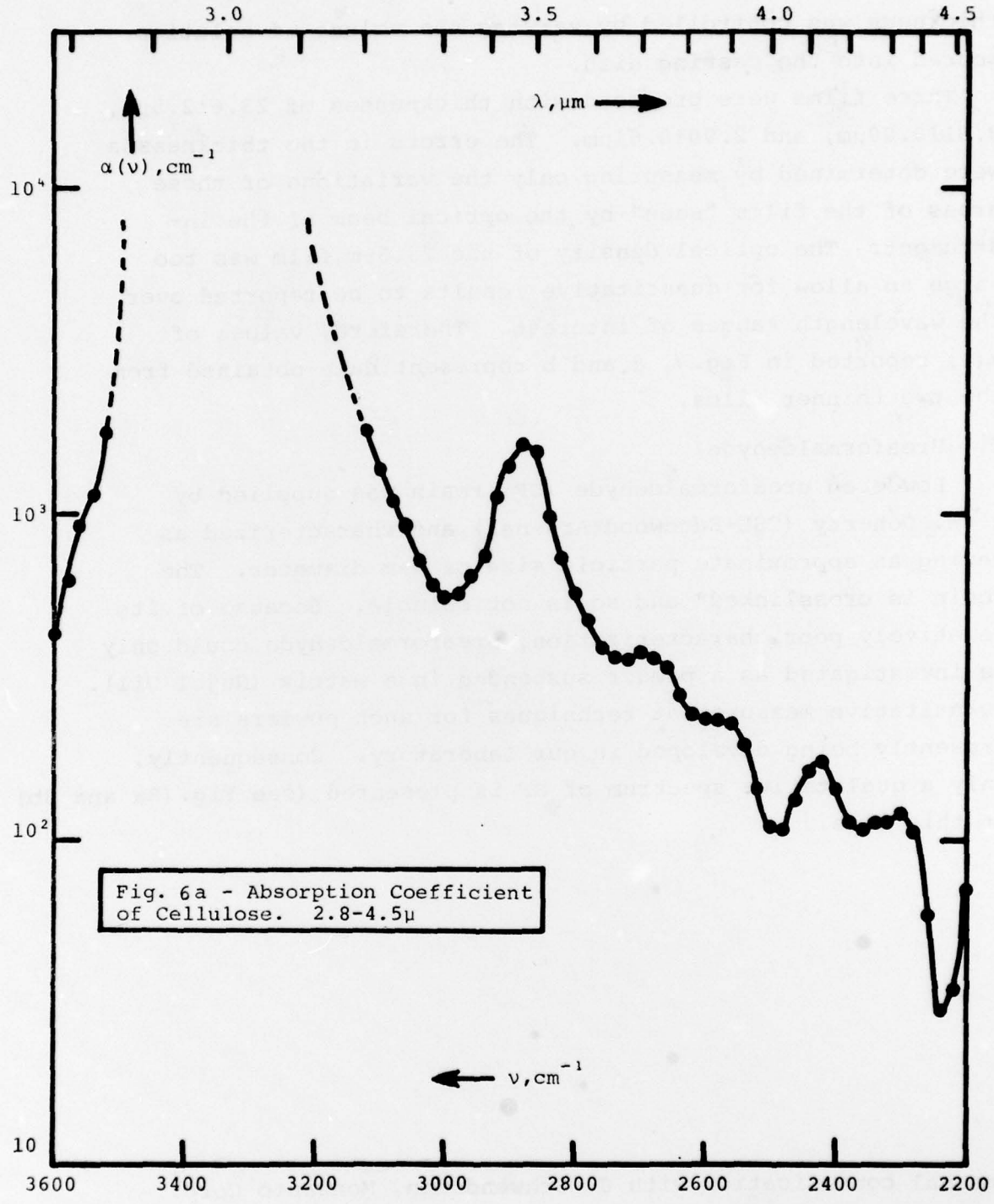

Fig. 6a - Absorption Coefficient of Cellulose. 2.8-4.5μ

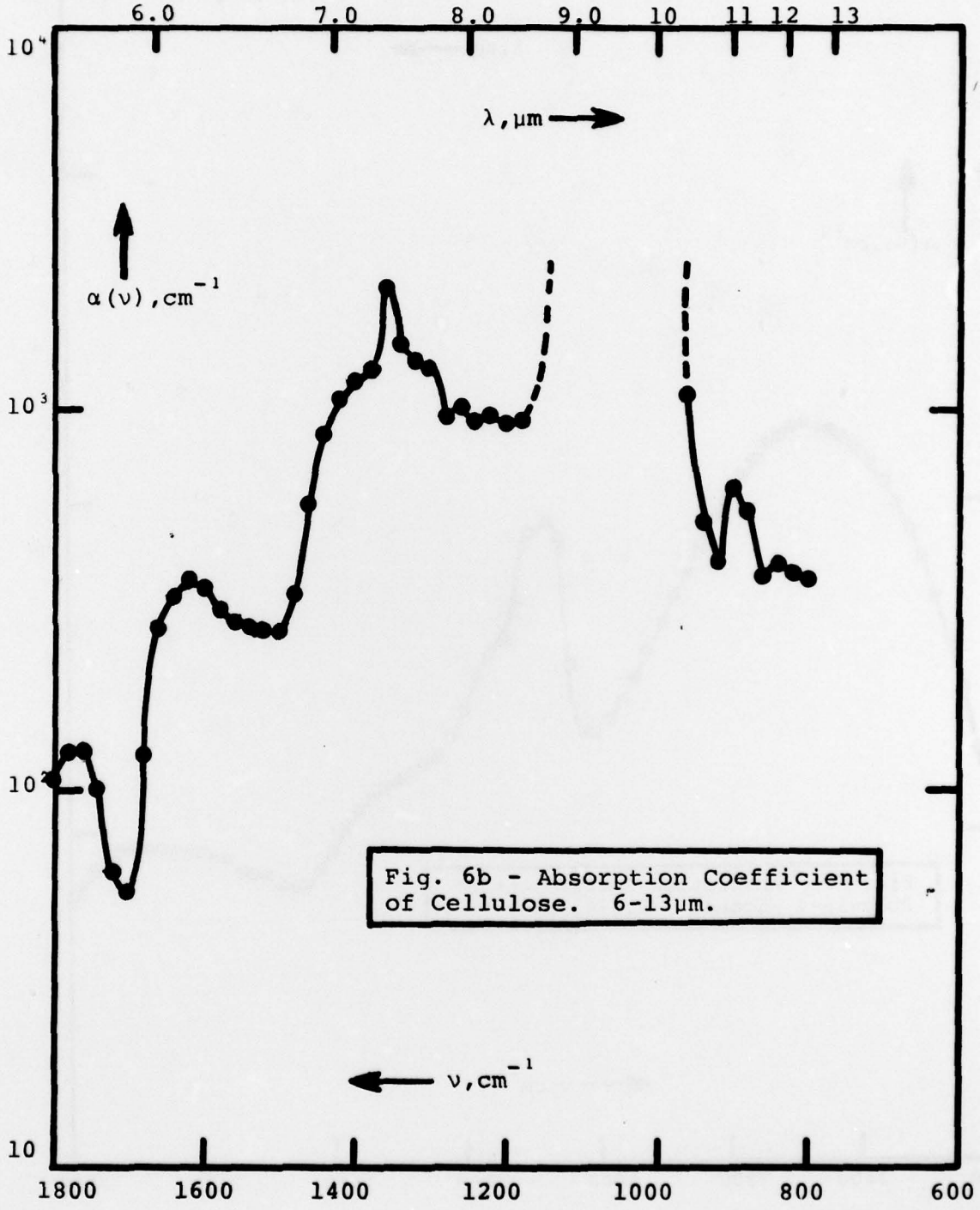

Fig. 6b - Absorption Coefficient of Cellulose. 6-13μm.

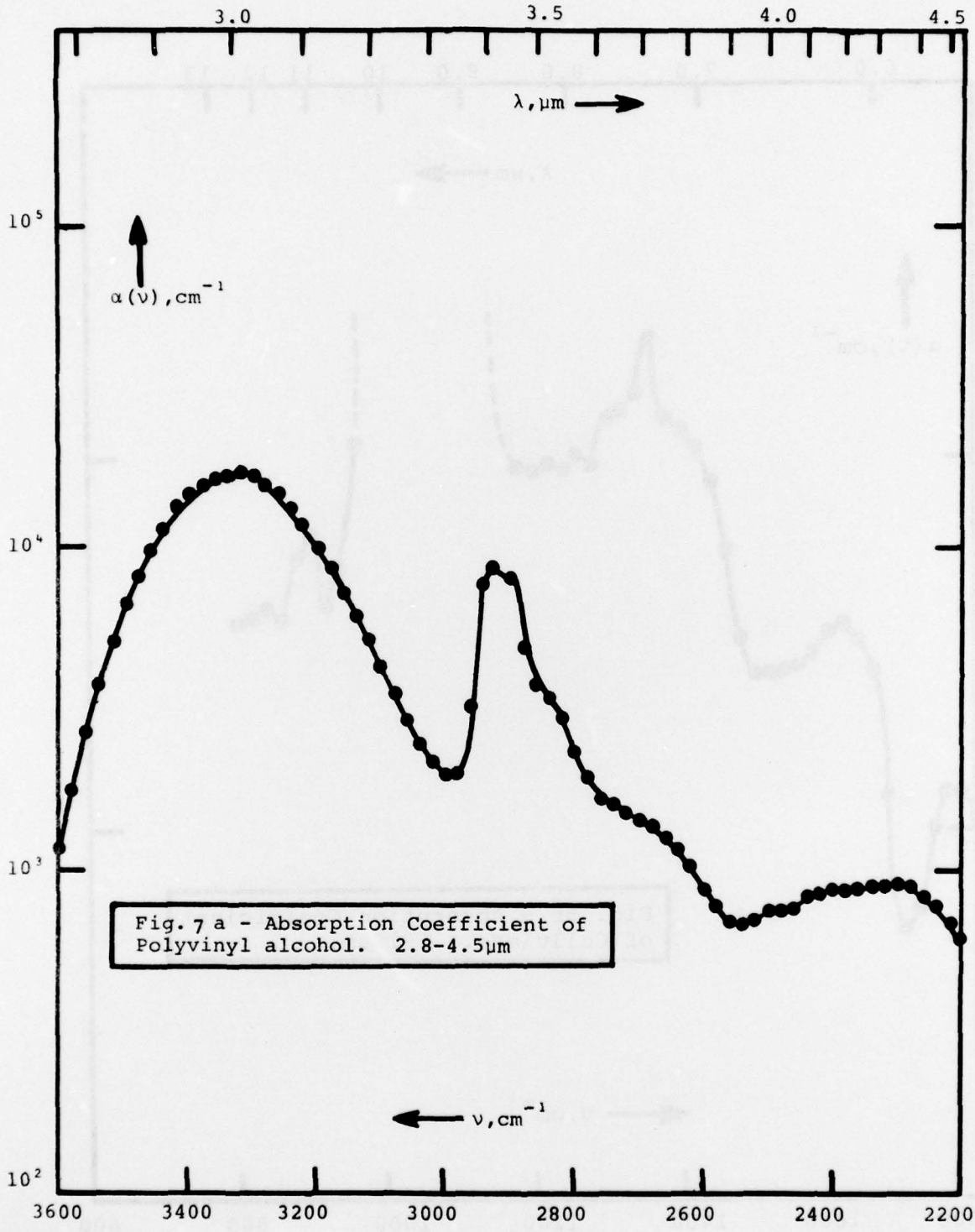

Fig. 7 a - Absorption Coefficient of Polyvinyl alcohol. 2.8-4.5μm

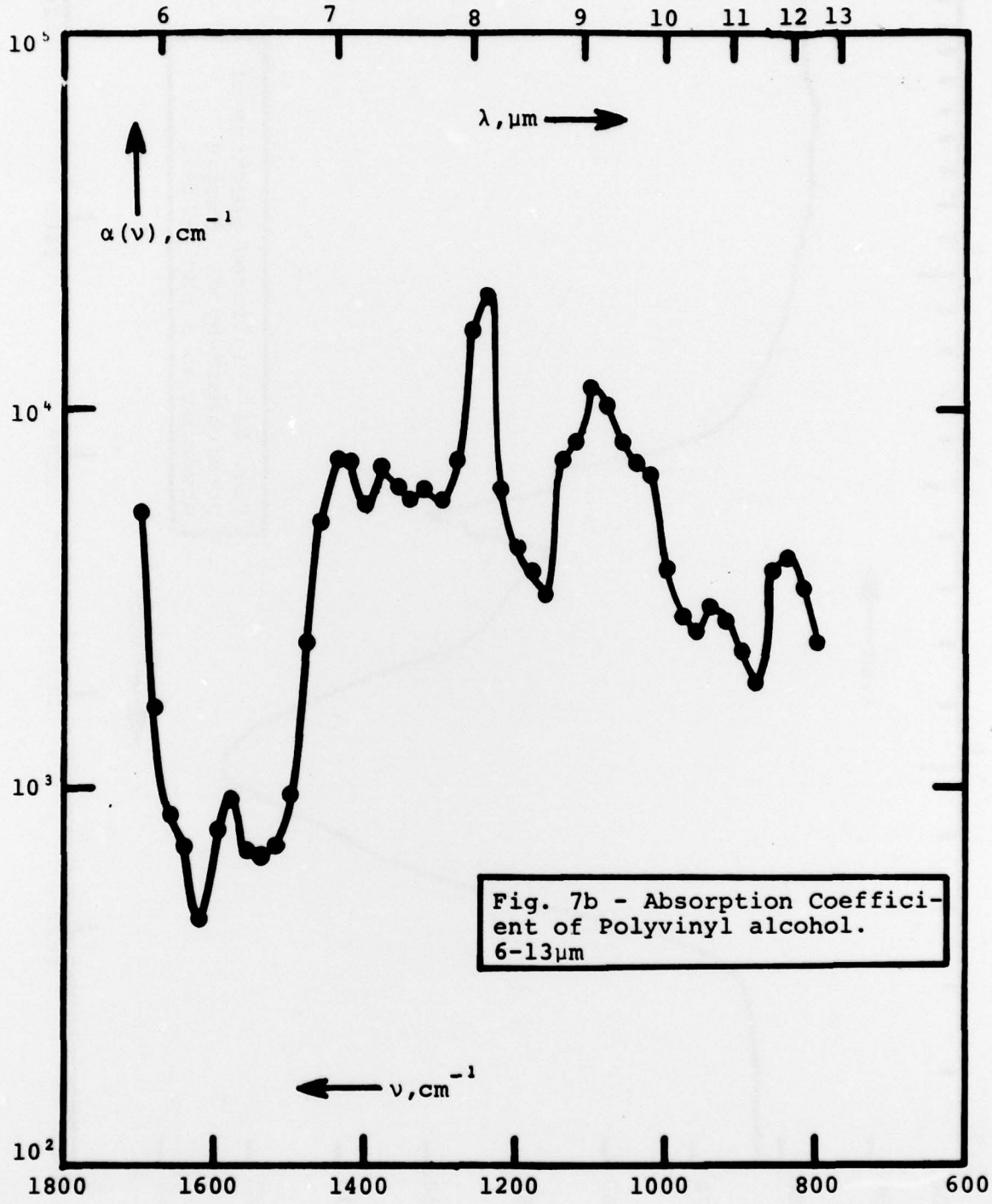

Fig. 7b - Absorption Coefficient of Polyvinyl alcohol. 6-13μm

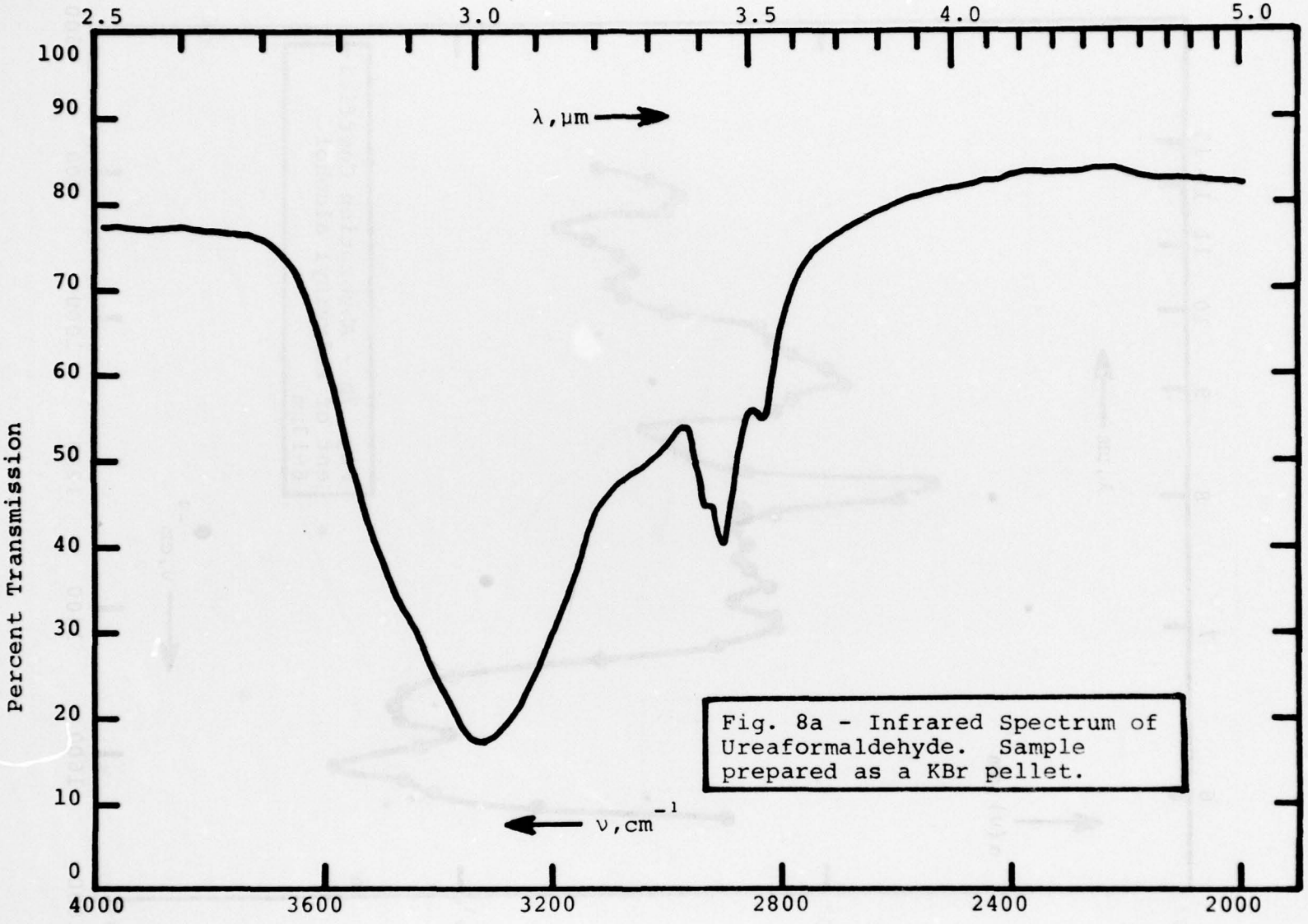

Fig. 8a - Infrared Spectrum of Ureaformaldehyde. Sample prepared as a KBr pellet.

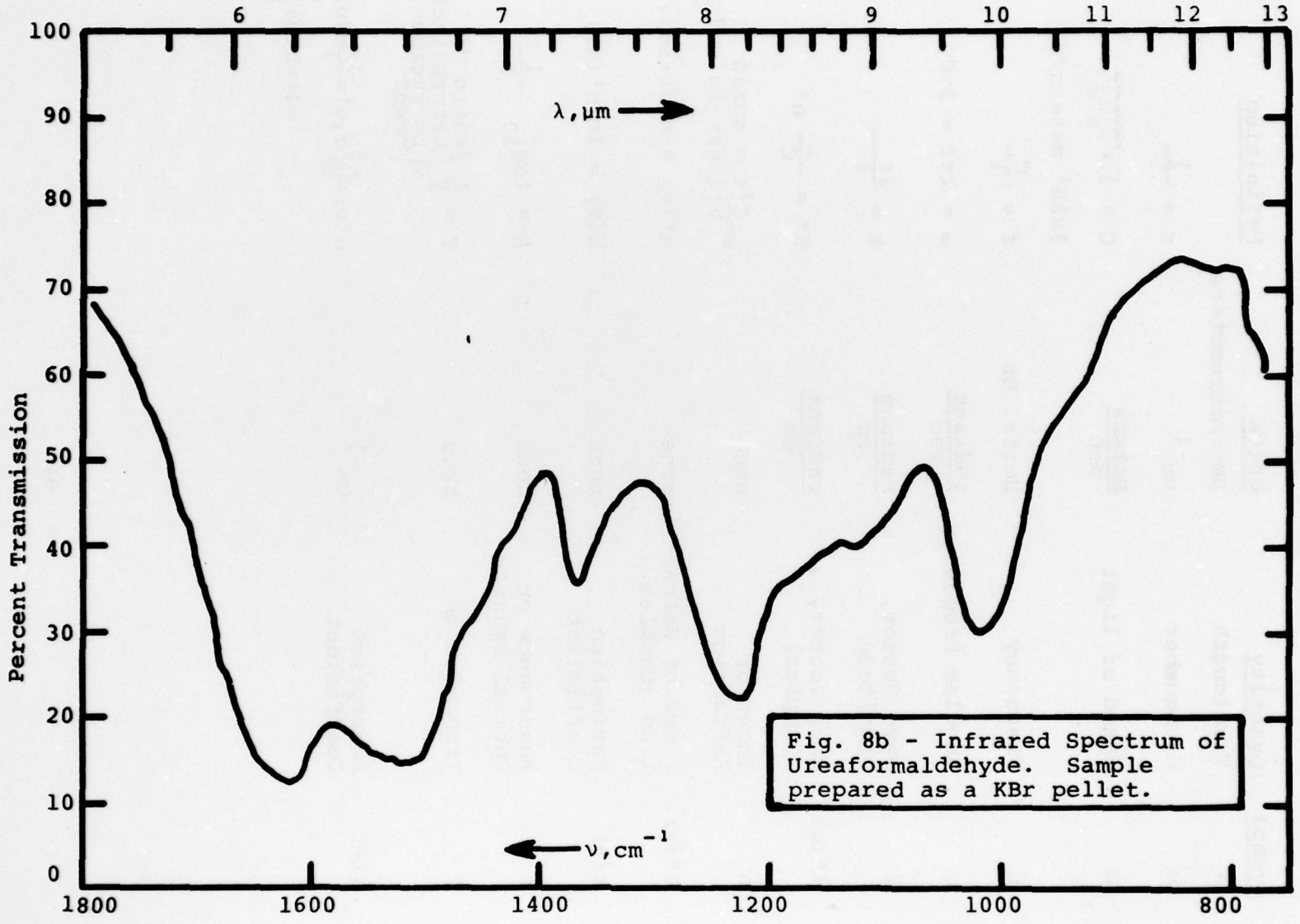

Fig. 8b - Infrared Spectrum of Ureaformaldehyde. Sample prepared as a KBr pellet.

GLOSSARY OF SELECTED TERMS

Symbol	Quantity	Units	Definition
λ	Wavelength	$\mu m \equiv$ micrometers	
ν	Wavenumber	cm^{-1}	$\nu = \frac{1}{\lambda}$
C	Speed of light	$\frac{\text{meters}}{\text{sec}}$	$C = 1/\sqrt{\varepsilon_o \mu_o} =$ 3×10^8 meters/s
f	Frequency	Hertz, Hz	$f = \frac{C}{\lambda}$
ω	Angular Frequency	$\frac{\text{radians}}{\text{sec}}$	$\omega = 2\pi f = 2\pi C\nu$
K	Wave Vector, Magnitude	$\frac{\text{radians}}{\text{cm}}$	$K = \frac{2\pi}{\lambda}$
$K^*(\omega)$	Wave Vector, (Complex)	$\frac{\text{radians}}{\text{cm}}$	$K^* = \frac{\omega}{C} n^*$
n	Index of Refraction	none	$n = \frac{C}{V}$ (V = speed of light in medium)
$n^*(\nu)$	Index of Refraction (Complex)	none	$n^*(\nu) = n(\nu) + ik(\nu)$
$k(\nu)$	Extinction Coefficient	none	$k(\nu) = Im[n^*(\nu)]$
A	Absorbance or Optical Density	none	$A = \log_{10} \frac{1}{T}$
T	Transmission	none	$T = \frac{I}{I_o}$ (ratio of transmitted to incident power)
$\alpha(\nu)$	Absorption Coefficient	cm^{-1}	$\alpha(\nu) = \frac{A}{B}$ ($\alpha(\nu) = \frac{4\pi}{\lambda} k(\nu) = 4\pi\nu k(\nu)$)

Symbol	Quantity	Units	Definition
b	Optical Path Length	cm	
$\varepsilon(\nu)$	Molar Extinction Coefficient	$\frac{\text{liter}}{\text{mole-cm}}$	$\varepsilon(\nu) = \frac{A}{bc}$ $\left[\varepsilon(\nu) = \frac{4\pi}{c}\nu k(\nu)\right]$
c	Concentration	$\frac{\text{mole}}{\text{liter}}$	

Appendix A: Development of General Wave Equation to Describe The Propagation of Light in Dielectric or Conductive Media.

The behavior of electromagnetic waves in any medium is described by the classical wave equation, which in turn is derived from Maxwell's Equations. In this section the development of the appropriate wave equation, of interest to this work, will be briefly presented.

The material parameters used to characterize the medium with respect to electromagnetic phenomena are, in SI units, the relative permitivity $\kappa_e = \varepsilon/\varepsilon_o$ ($\varepsilon_o = 8.85 \times 10^{-12}$ farad m^{-1} = permitivity of free space) and the relative permeability $\kappa_m = \mu/\mu_o$ ($\mu_o = 1.26 \times 10^{-6}$ henry m^{-1} = permeability of free space). The velocity of propagation of the wave in this medium is

$$V = \frac{1}{\sqrt{\varepsilon\mu}} = \frac{1}{\sqrt{\kappa_e \varepsilon_o \kappa_m \mu_o}} \qquad \text{(A-1)}$$

which, for free space (in vacuo $\kappa_e = \kappa_m = 1$) reduces to

$$C = \sqrt{\frac{1}{\varepsilon_o \mu_o}} \simeq 3 \times 10^8 \text{ m/s} \qquad \text{(A-2)}$$

The index of refraction of the medium is given by

$$u = \frac{C}{V} = \sqrt{\kappa_e \kappa_m} \qquad \text{(A-3)}$$

For most transparent optical media $\kappa_m = 1$ so that

$$n = \sqrt{\kappa_e} = \sqrt{\varepsilon/\varepsilon_o} \qquad \text{(A-4)}$$

This result is generally only valid for dilute gases and non-polar solids, where high static polarizability is present. In

addition, n is a function of frequency (dispersion) so that to characterize the medium optically, these effects must be accounted for and (A-4) is seen to be a special limiting case.

Maxwell's Equations for a non-magnetic, electrically neutral medium can be reduced to

$$\nabla \times \vec{E} = - \mu_o \frac{\partial \vec{H}}{\partial t} \tag{A-5a}$$

$$\nabla \times \vec{H} = \varepsilon_o \frac{\partial \vec{E}}{\partial t} + \frac{\partial \vec{P}}{\partial t} + \vec{j} \tag{A-5b}$$

$$\nabla \cdot \vec{E} = - \frac{1}{\varepsilon_o} \nabla \cdot \vec{P} \tag{A-5c}$$

$$\nabla \cdot \vec{H} = 0 \tag{A-5d}$$

where $\vec{E}$ is the electric field intensity, $\vec{H}$ is the magnetic field intensity,

$$\vec{P} = (\varepsilon - \varepsilon_o) E = \chi \varepsilon_o \vec{E} \tag{A-6}$$

is the electric polarization ($\chi = \frac{\varepsilon}{\varepsilon_o} - 1$ = electric susceptability) and

$$\vec{j} = \sigma \vec{E} \tag{A-7}$$

is the current density (σ = electrical conductivity).

By manipulating the above equations [take the curl of (A-5a) and time derivative of (A-5b) and eliminate $\vec{H}$ between the two resulting equations] one can get

$$\nabla \times (\nabla \times \vec{E}) + \frac{1}{C^2} \frac{\partial^2 \vec{E}}{\partial t^2} = - \mu_o \frac{\partial^2 \vec{P}}{\partial t^2} = - \mu_o \frac{\partial \vec{j}}{\partial t} \tag{A-8}$$

From the vector identity

$$\nabla \times (\nabla \times \vec{E}) = \nabla (\nabla \cdot \vec{E}) - \nabla^2 \vec{E} \tag{A-9}$$

and the fact that $\nabla \cdot \vec{E} = 0$ for an electrically neutral media, it follows that

$$\nabla^2 \vec{E} - \frac{1}{c^2} \frac{\partial^2 \vec{E}}{\partial t^2} = \mu_o \frac{\partial^2 \vec{P}}{\partial t^2} + \mu_o \frac{\partial \vec{j}}{\partial t} \qquad \text{(A-10)}$$

The two terms on the right hand side of (A-10) are called source terms and are interpreted as follows:

(a) For a non-conducting medium, $\frac{\partial^2 \vec{P}}{\partial t^2}$ accounts for the effect of polarization charges and is the important source term, being responsible for optical effects such as dispersion, absorption, etc.

(b) For a conducting medium, $\frac{\partial \vec{j}}{\partial t}$ is the important term and is responsible for the high reflectivity and optical opacity of metals.

(c) For semiconductors, both source terms must be considered.

Equation (A-10) is the starting point for discussions of dispersion and metallic absorption considered in this work.

DISTRIBUTION LIST FOR ARCSL-CR-79052

Names	Copies
Chemical Systems Laboratory Aberdeen Proving Ground, MD 21010	
Office of the Director Attn: DRDAR-CLG	1
CB Detection & Alarms Division Attn: DRDAR-CLC	1
Developmental Support Division Attn: DRDAR-CLJ-L Attn: DRDAR-CLJ-R Attn: DRDAR-CLJ-M	3 2 1
Munitions Division Attn: DRDAR-CLN Attn: DRDAR-CLN-S	1 1
Physical Protection Division Attn: DRDAR-CLW-P	1
Research Division Attn: DRDAR-CLB Attn: DRDAR-CLB-B Attn: DRDAR-CLB-P Attn: DRDAR-CLB-T Attn: DRDAR-CLB-PS (Mr. Vervier) Attn: DRDAR-CLB-PS (Dr. Stuebing) Attn: DRDAR-CLB-PS (Mr. Frickel)	1 1 1 1 1 10 1
Systems Development Division Attn: DRDAR-CLY-A Attn: DRDAR-CLY-R	1 6
DEPARTMENT OF DEFENSE	
Administrator Defense Documentation Center Attn: Document Processing Division (DDC-DD) Cameron Station Alexandria, VA 22314	12
Office of the Director Defense Research and Engineering Attn: Dr. T.C. Walsh, Rm 3D-1079 Washington, DC 20310	1
Institute for Defense Analysis 400 Army-Navy Drive Attn: L. Biberman Attn: R. E. Roberts Arlington, VA 22202	1 1
Advanced Research Projects Agency 1400 Wilson Boulevard Arlington, VA 22209	1

Names	Copies
DEPARTMENT OF THE ARMY	
Commander US Army Research Office – Durham Box CM, Duke Station Durham, NC 27706	1
HQDA (DAMO-SSC) HQDA (DAMA-ARZ, Dr. Verderame) HQDA (DAMA-CSM-CM) HQDA (DAMI-FIT) WASH DC 20310	1 1 1 1
US ARMY MATERIEL DEVELOPMENT AND READINESS COMMAND	
Commander US Army Materiel Development and Readiness Command Attn: DRCDE-DM Attn: DRCLDC Attn: DRCMT Attn: DRCSF-S Attn: DRCDL (Mr. N. Klein) Attn: DRCBI (COL Gearin) Attn: DRCDMD-ST (Mr. T. Shirata) 5001 Eisenhower Ave. Alexandria, VA 22333	1 1 1 1 1 1 1
Commander US Army Foreign Science & Technology Center Attn: DRXST-MT-2 Attn: DRXST-CE (Mr. V. Rague) 220 Seventh St., NE Charlottesville, VA 22901	1 1
Commander US Army Missile Command Redstone Scientific Information Center Attn: Chief, Documents Attn: DRDMI-CGA (Dr. B. Fowler) Attn: DRDMI-TE (Mr. H. Anderson) Attn: DRDMI-KL (Dr. W. Wharton) Redstone Arsenal, AL 35809	1 1 1 1
US ARMY ARMAMENT RESEARCH AND DEVELOPMENT COMMAND	
Commander US Army Armament Research and Development Command Attn: DRDAR-TSS Dover, NJ 07801	5
US ARMY ARMAMENT MATERIEL READINESS COMMAND	
Commander US Army Armament Materiel Readiness Command Attn: DRSAR-ASN Attn: DRSAR-PE Rock Island, IL 61299	1 1

DISTRIBUTION LIST FOR ARCSL-CR-79052 (Contd)

Names	Copies
Commander Harry Diamond Laboratories Attn: DRXDO-RDC (Mr. D. Giglio) 2800 Powder Mill Road Adelphi, MD 20783	1
Chief, Office of Missile Electronic Warfare US Army Electronic Warfare Laboratory Attn: DRSEL-WLM-SE (Mr. K. Larson) White Sands Missile Range, NM 88002	1
Project Manager for Smoke/Obscurants Attn: DRCP-SMK Aberdeen Proving Ground, MD 21005	2
Commander Atmospheric Sciences Laboratory Attn: DRSEL-BR-AS-P Attn: DRSEL-BR-MS-A (Dr. R. Gomez) Attn: DRSEL-BL-AS-DP (Mr. J. Lindberg) Attn: DRSEL-BL-SY (Mr. F. Horning) White Sands Missile Range, NM 88002	1 1 1 1
Director US Army Materiel Systems Analysis Activity Attn: DRXSY-D (Dr. Fallin) Attn: DRXSY-MP Aberdeen Proving Ground, MD 21005	1 1
Director Night Vision Laboratories Attn: DRSEL-NV-VI (Mr. R. Moulton) Attn: DRSEL-NV-VI (Mr. R. Bergemann) Fort Belvoir, VA 23651	1 1
US Army Mobility Equipment Research and Development Center Attn: Code/DROME-RT (Mr. O. F. Kezer) Fort Belvoir, VA 22060	1
Commander US Army Electronics Command Attn: DRSEL-CT-LG (Dr. R. G. Rohde) Attn: DRSEL-CT-I (Dr. R. G. Buser) Attn: DRSEL-WL-S (Mr. J. Charlton) Fort Monmouth, NJ 07703	1 1 1
Director US Army Ballistic Research Laboratories Attn: DRXBR-DL (Mr. T. Finnerty) Attn: DRXBR-P (Mr. N. Gerri) Attn: DRDAR-BLB (Mr. R. Reitz) Attn: DRDAR-BLB (Mr. A. LaGrange) Aberdeen Proving Ground, MD 21005	1 1 1 1
CDR, APG Attn: STEAP-AD-R/RHA Attn: STEAP-TL Aberdeen Proving Ground, MD 21005	1 1
Commander US Army Test & Evaluation Command Attn: DRSTE-FA Aberdeen Proving Ground, MD 21005	1
Commander Dugway Proving Ground Attn: STEDP-PO Attn: Technical Library, Docu Sec Attn: STEDP-MT-DA-E Attn: STEDP-MT (Dr. L. Salamon) Dugway, UT 84022	1 1 1 1
US ARMY TRAINING & DOCTRINE COMMAND	
Commandant US Army Infantry School Combat Support & Maintenance Dept Attn: NBC Division Fort Benning, GA 31905	1
Commandant US Army Missile & Munitions Center & School Attn: ATSK-CD-MD Attn: ATSK-DT-MU-EOD Redstone Arsenal, AL 35809	1 1
Commander US Army Logistics Center Attn: ATCL-MM Fort Lee, VA 23801	1
Commander HQ, USA TRADOC Attn: ATCD-TEC (Dr. M. Pastel) Fort Monroe, VA 23651	1
Commander US Army Ordnance & Chemical Center & School Attn: ATSL-CD-MS Attn: ATSL-CD-MS (Dr. T. Welsh) Aberdeen Proving Ground, MD 21005	1 1
DEPARTMENT OF THE NAVY	
Commander Naval Surface Weapons Center Attn: Tech Lib & Info Svcs Br White Oak Laboratory Silver Spring, MD 20910	1
Commander Naval Intelligence Support Center 4301 Suitland Road Washington, DC 20390	1
Commander Naval Surface Weapons Center Dahlgren Laboratory Attn: DX-21 Dahlgren, VA 22448	1

Names	Copies
Commander	
Naval Weapons Center	
Attn: Code 3311 (Dr. R. Bird)	1
Attn: Code 382 (Dr. P. St. Amand)	1
Attn: Code 3822 (Dr. Hindman)	1
China Lake, CA 93555	
Commanding Officer	
Naval Weapons Support Center	
Attn: Code 5041 (Mr. D. Johnson)	1
Attn: Code 5042 (Mr. C. Dinerman)	1
Crane, IN 47522	
Commander	
Naval Research Laboratory	
Attn: Code 5709 (Mr. W. E. Howell)	1
4555 Overlook Avenue, SW	
Washington, DC 20375	

Names	Copies
DEPARTMENT OF THE AIR FORCE	
HQ, Foreign Technology Division (AFSC)	
Attn: PDRR	1
Wright-Patterson AFB, OH 45433	
Commander	
Armament Development & Test Center	
Attn: DLOSL (Technical Library)	1
Eglin AFB, FL 32542	
Commander	
USEUCOM	
Attn: ECJ5-O/LTC James H.Alley	1
APO, NY 09128	
USA BIOMEDICAL LABORATORY	
Attn: SGRD-UV-ZA	1